1 **Title** High-throughput feedback-enabled optogenetic stimulation and spectroscopy in microwell plates

2

3 **Authors:** William Benman[1,†], Saachi Datta[1,†], David Gonzalez-Martinez[1], Gloria Lee[1], Juliette Hooper[1], Grace

4 Qian[1], Gabrielle Leavitt[1], Lana Salloum[1], Gabrielle Ho[1], Sharvari Mhatre[1], Michael S. Magaraci[1], Michael

5 Patterson[1], Sevile G. Mannickarottu[1], Saurabh Malani[2], Jose L. Avalos[2,3,4], Brian Y. Chow[1], Lukasz J.

6 Bugaj[1,5,6]*

7

8 **Affiliations:**

9

10 [1]Department of Bioengineering, University of Pennsylvania, Philadelphia, PA, 19104, USA

11 [2]Department of Chemical and Biological Engineering, Princeton University, Princeton, NJ 08544

12 [3]The Andlinger Center for Energy and the Environment, Princeton, NJ 08544

13 [4]High Meadows Environmental Institute, Princeton, NJ 08544

14 [5]Abramson Cancer Center, University of Pennsylvania, Philadelphia, PA, 19104, USA

15 [6]Institute of Regenerative Medicine, University of Pennsylvania, Philadelphia, PA, 19104, USA

16

17

18

19 [†]equal contribution

20 *corresponding author

21

22 **Correspondence:** bugaj@seas.upenn.edu

23

24

25

26

27

28

29 **ABSTRACT**

30 The ability to perform sophisticated, high-throughput optogenetic experiments has been greatly enhanced by

31 recent open-source illumination devices that allow independent programming of light patterns in single wells of

32 microwell plates. However, there is currently a lack of instrumentation to monitor such experiments in real time,

33 necessitating repeated transfers of the samples to stand-alone analytical instruments, thus limiting the types of

34 experiments that could be performed. Here we address this gap with the development of the optoPlateReader

35 (oPR), an open-source, solid-state, compact device that allows automated optogenetic stimulation and

36 spectroscopy in each well of a 96-well plate. The oPR integrates an optoPlate illumination module with a

37 module called the optoReader, an array of 96 photodiodes and LEDs that allows 96 parallel light

38 measurements. The oPR was optimized for stimulation with blue light and for measurements of optical density

39 and fluorescence. After calibration of all device components, we used the oPR to measure growth and to

40 induce and measure fluorescent protein expression in *E. coli*. We further demonstrated how the optical

41 read/write capabilities of the oPR permit computer-in-the-loop feedback control, where the current state of the

42 sample can be used to adjust the optical stimulation parameters of the sample according to pre-defined

43 feedback algorithms. The oPR will thus help realize an untapped potential for optogenetic experiments by

44 enabling automated reading, writing, and feedback in microwell plates through open-source hardware that is

45 accessible, customizable, and inexpensive.

46

47 **MAIN TEXT**

48

49 **Introduction**

50 Optogenetic tools allow precise control of molecular activity inside cells using light as a stimulus. Because light
51 can be readily interfaced with computers, optogenetic experiments are highly amenable to automation.
52 Recently, due to the accessibility of small and programmable light sources, integrated circuits, and additive
53 manufacturing, several groups have developed custom devices to miniaturize and parallelize optogenetic
54 experiments[1–9]. These devices comprise arrays of light-emitting diodes (LEDs) positioned in the format of
55 standard biological multi-well plates, often controllable by open-source hardware and software (e.g. Arduino,
56 Python). Collectively, such devices allow programmable, high-throughput control of biological systems
57 including in bacteria, yeast, mammalian cells, and other model organisms, with up to 3 stimulation colors per
58 well. They are also inexpensive, often costing well below $1000 to construct. As a result, open-source devices
59 for high-throughput optogenetics help realize the high potential of optogenetics for systematic, data-rich, and
60 robust experiments without the need for complex robotics or bespoke microfluidics.

61

62 Despite the proliferation of such hardware, there is a lack of devices that also allow simultaneous
63 measurement of the samples, for example through spectroscopy. Simultaneous stimulation and measurement
64 in one integrated device would be highly enabling. First, it would streamline optogenetic experiments, removing
65 the need for manually transferring the sample plate from the stimulation device to a plate reader or
66 microscope, allowing higher resolution time sampling and removing sources of experimental error, such as
67 unwanted light exposure while transferring samples. Second, real-time measurement and perturbation would
68 allow computer-in-the-loop feedback control, where the stimulation can be adjusted based on the current state
69 of the sample. Such control could have many uses, for example for optimizing optogenetically controlled
70 metabolic pathways in which enzymes are expressed at precise levels and only during a particular phase of
71 cell culture growth[10]. Although all-optical feedback control has been previously implemented, it has required
72 expensive microscopes[11,12] or customization of flow cytometers[13,14] and could only act on one sample at a time.
73 Recently, custom devices were reported that allowed optogenetic stimulation and imaging of bacterial cultures
74 in microwell plates[15] or in batch culture[16]. However, these devices were limited to experiments in four wells or
75 one bulk culture, respectively.

76

77 In recent years, open-source spectrophotometers have been described that could in principle be coupled with
78 illumination devices. Richter et al demonstrated that a Tecan plate reader could be retrofitted for optogenetic
79 stimulation by converting the on-board fluidics machinery to position an LED-coupled optical fiber above
80 predefined wells[17]. However, this approach could only read and write from one sample at a time and required
81 access to a Tecan plate reader that could be customized. Separately, Szymula et al described the open-source
82 plate reader (OSP), which provides full-spectrum absorbance and fluorescence detection in microwell plates
83 and allows optogenetic stimulation and reading of an individual well[18]. However, this instrument could not
84 regulate sample temperature and thus could not support continuous cell culture, and also required sequential
85 stimulation/measurement of each well. Jensen et al developed a 96-well solid-state plate-reader that used an
86 array of 96 phototransistors to optically measure each well independently[19]. This device could measure light
87 from all wells simultaneously and could be shaken and multiplexed within bacterial incubators. However, it
88 could only measure OD but not fluorescence, and could not be used to stimulate optogenetic systems.

89

90 In this work, we describe the development of the optoPlateReader (oPR), an integrated device that allows 96
91 parallel channels of optical stimulation, measurement of fluorescence and optical density, and feedback control
92 of stimulation based on real-time measurements of biological samples. We characterize the detection limits of
93 our device and demonstrate its ability to measure bacterial growth and arabinose- or light-inducible expression

94   of the fluorescent protein mAmetrine with low variability between wells. Finally, we demonstrate that 96
95   separate cultures can be independently and simultaneously regulated to control gene expression programs in
96   real time conditional on the current growth or expression state of the sample.
97
98   **Results**
99   *Design of optoPlateReader for simultaneous optogenetic reading and writing*
100   The optoPlateReader (oPR) was designed for high-throughput light stimulation with real-time fluorescence and
101   absorbance measurements in a 96-well plate format. Other important specifications included 1) a small
102   footprint such that the device could be placed into a standard cell culture incubator for environmental control,
103   2) stable mechanical and electrical connections for robustness and to allow shaking, 3) integration between
104   measurement and stimulation to allow for autonomous feedback control, 4) a user interface that allowed easy
105   programming of all experimental parameters.
106
107   The oPR is composed of two separate device modules: the optoPlate, which provides light sources for
108   optogenetics and OD readings, and the optoReader, which provides components for optical measurement and
109   light sources for fluorescence excitation (**Figure 1A**). All stimulation and measurement can be controlled
110   independently for each of the 96 separate wells. Both device modules consist of a custom-designed printed
111   circuit board (PCB) assembled with surface-mounted semiconductor components. Surface-mounted
112   components can be small in size, allow for rapid and precise device assembly without the need for specialized
113   equipment or expertise in hand soldering (See **Methods** and **design files),** and offer the potential for scalable
114   production. A clear-bottom, opaque-walled 96-well sample plate is positioned between the optoPlate (top) and
115   the optoReader (bottom) modules. Both modules are fitted with 3D-printed adapters that securely mate the
116   circuit boards to the sample plate. The small format of the assembled oPR allows it to fit within cell culture
117   incubators, and the lack of moving parts and wires provides robustness, for example allowing the device to be
118   shaken. For shaking, the oPR can be mounted on a microplate orbital shaker. The oPR can communicate with
119   the shaker via a 5V relay, allowing shaking to be paused during measurements and resumed after
120   measurements are complete. For environmental control, the device assembly can be placed inside of a
121   standard 37°C cell culture incubator.
122
123   The optoPlate is derived from a previously reported optogenetic stimulation device, the optoPlate-96[1]. The
124   optoPlate consists of 96 pairs of LEDs, arranged such that each pair of LEDs illuminates a single well of a 96-
125   well plate. We adapted this device to rest on top of the sample well plate, and we selected LED pairs to allow
126   both optogenetic stimulation (470 nm) and optical density readings (600 nm). We selected bi-color blue/red
127   LEDs for optogenetic stimulation because the majority of current optogenetic tools respond to blue or red light,
128   though we exclusively used blue light for optogenetic stimulation in this study. The bi-color LED can be
129   replaced with a mono- or bi-color LED of any wavelength for custom applications, provided that the LED form
130   factor is compatible with the optoPlate PCB (either PLCC2 or PLCC4). A 3D-printed adapter is mounted on the
131   optoPlate to securely mate and align the optoPlate with the sample plate. The intensity of all LEDs is regulated
132   via pulse width modulation (PWM) enabling 4095 levels of intensity control.
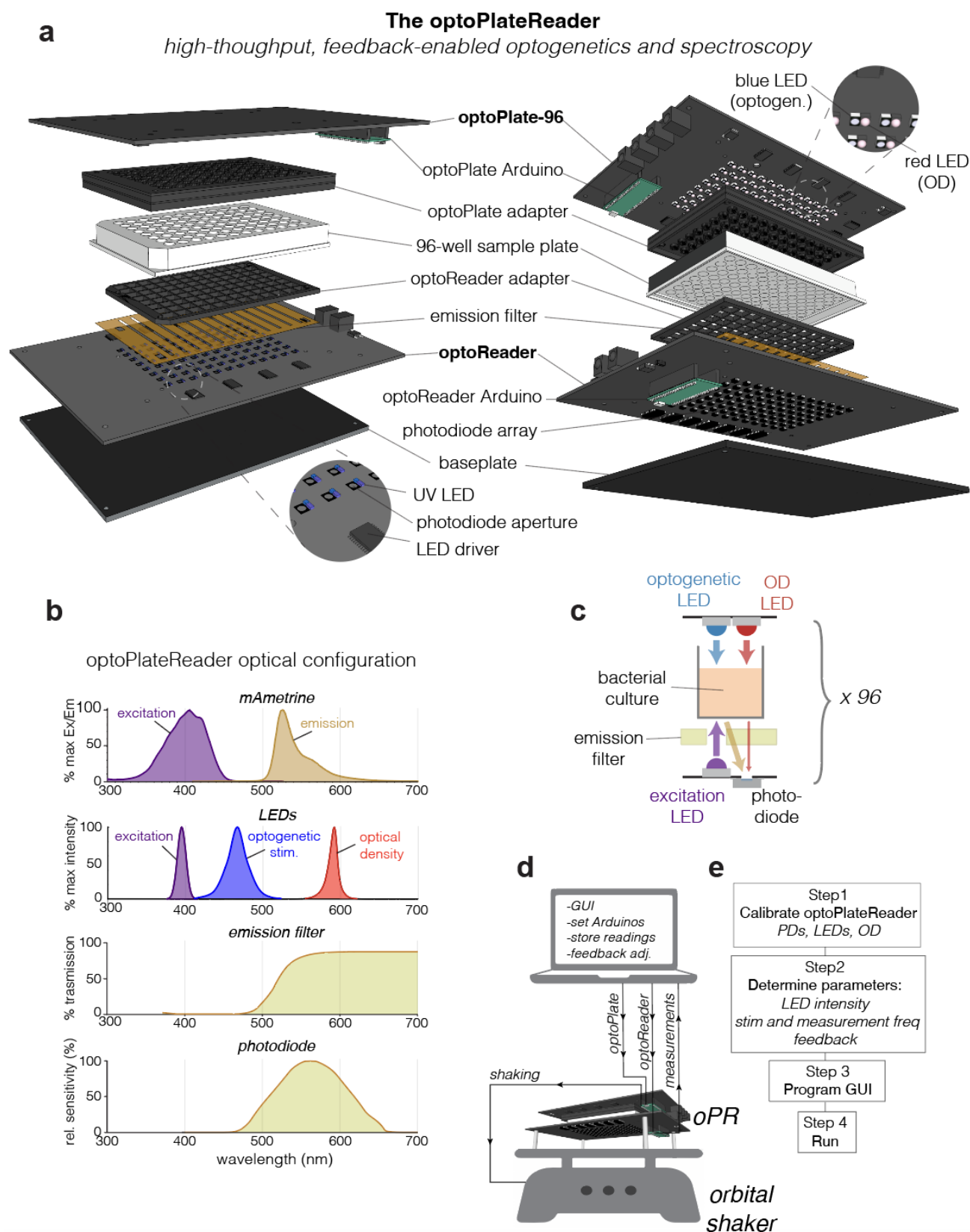
Figure 1. The optoPlateReader (oPR) enables high throughput optical stimulation and spectroscopy in a 96-well format. a Exploded view of the oPR. The optoPlate-96 and optoReader each feature an array of 96 LEDs or photodiodes that independently optically stimulate and measure each well of a 96-well plate. The 3D-printed adaptors provide light insulation between wells and provide a tight mating to a black-walled, clear-

138   bottom 96-well plate. **b** Optical spectra for mAmetrine and the oPR components, which were selected to
139   maximize detection of fluorescence emission and absorbance measurements while preventing detection of
140   excitation light. **c** Schematic of optical stimulation and measurement of a single well in the oPR. **d**
141   Communication of a computer with the oPR during an experiment. The computer receives user input and real-
142   time measurements from the oPR, calculates updates to stimulation parameters based on feedback
143   algorithms, and sends commands and updated protocols to the optoPlate and optoReader Arduinos. The
144   optoReader Arduino sends photodiode measurements back to the computer. Communication between the oPR
145   and an orbital shaker allows for sample agitation between measurements. **e** Overview of workflow for oPR
146   demonstrating steps a user must take after oPR construction and before performing an experiment. Note that
147   whereas calibration of blue LEDs, UV LEDs, and photodiodes needs to be performed once, calibration of OD
148   measurements (red LEDs) must be performed before each experiment.

149

150 The optoReader is a solid state, 96-well fluorescence plate reader (**Figure 1A)**. The optoReader contains 96
151 pairs of one photodiode and one UV LED, arrayed in 96-well format. The photodiodes are the light-sensing
152 element used to measure fluorescence and OD. The optical configuration of the oPR has been optimized to
153 measure fluorescence of mAmetrine. mAmetrine is a derivative of GFP with a long Stokes shift[20]— that is, with
154 a relatively large difference between its excitation and emission wavelength (**Figure 1B, top**). The long Stokes
155 shift allows the excitation light (UV) to be efficiently filtered out while maximally preserving the emission light
156 using only inexpensive filters (see below and **Methods**). An additional benefit of mAmetrine is that its excitation
157 spectrum minimally overlaps with the blue LED spectrum, minimizing bleaching of the fluorescent protein from
158 optogenetic stimulation (**Figure 1B**). To excite mAmetrine, we used a near-UV LED (395 nm) positioned next
159 to each photodiode. To filter out UV excitation light from the photodiode detector, we implemented emission
160 filters above all photodiodes using canary yellow camera filters (Rosco Roscolux) (**Figure 1A,B**). We cut
161 apertures in these filter films above the UV LEDs such that the UV light could be transmitted onto the sample,
162 but its reflection onto the photodiodes would be attenuated (**Figure 1C**). For further filtering, we selected
163 photodiodes that had minimal responsivity to light below 450 nm, further attenuating signal from the UV LED
164 while permitting detection of light from mAmetrine emission or the OD LED (**Figure 1B)**. For further possible
165 modification, the optoReader can also accommodate an additional LED component in each well position, if
166 desired, for example for detection of fluorescence from multiple fluorophores. As with the optoPlate, a 3D-
167 printed adapter mates the optoReader and the bottom of a 96-well plate, providing stability, light insulation
168 between wells, and alignment between all modules of the assembled oPR. Lack of light leakage between
169 wells, as well as spatial homogeneity of illumination, were experimentally confirmed (**Supplementary Figure
170 1**)

171

172 Both the optoPlate and optoReader modules are driven by on-board Arduino microcontrollers that
173 communicate with the local LEDs and photodiodes, with the central computer, and with the shaker. LEDs are
174 controlled by serial communication through 24-channel LED driver chips, as used previously[2]. To read 96
175 analog signals from all photodiodes, six 16-channel multiplexers take sequential readings from individually
176 addressable wells, and readings are transmitted to one analog input pin on the Arduino. For more details on
177 the optoReader circuitry, see **Supplementary Figure 2**. Both Arduinos communicate with a central computer
178 to send and receive commands through USB communication. The computer runs custom Python software that
179 sends illumination/measurement parameters to the Arduinos, coordinates timing (e.g. to ensure that
180 optogenetic stimulation does not occur during readings), and stores and processes measurements (**Figure
181 1D**). The oPR is able to record 96 fluorescence or OD readings in <1 min. The ability for the oPR to rapidly
182 measure a sample, perform calculations on those values, and dynamically update stimulation parameters
183 enables computer-in-the-loop feedback control, where optogenetic stimulation can be modified in real time
184 based on the current state of the sample. Such feedback control can be implemented in 96 independent
185 experiments at the same time.

186

187 We provide all design files and a parts list to print and assemble a fully functional oPR (See **Methods**). With
188 all components in hand, a fully-functional oPR can be assembled in ~6 hours for ~$700, with price decreasing
189 if components are purchased in larger quantities. After assembly, the general steps to perform an experiment
190 are as follows (**Figure 1E**): First, all oPR components must be calibrated to allow measurement and
191 stimulation with minimal variation between wells (see below). Second, the experimental cells must be grown
192 and plated, and the experimental conditions (stimulation intensity and frequency, measurement frequency)
193 must be determined. Third, the full oPR device with sample plate must be assembled and powered, the OD
194 readings must be calibrated, and the experimental parameters must be entered into the graphical user
195 interface (GUI). Finally, the experiment is initiated from the GUI. The following sections detail the oPR software

196 and calibration protocols and provide examples for the types of experiments that can be performed with the
197 oPR.
198 *The oPR software*
199 The oPR software allows the user to define all experimental parameters, coordinates the timing of all electronic
200 components, takes and stores measurements, and runs feedback algorithms to adjust stimulation parameters
201 based on predefined specifications (**Figure 2A**). The GUI allows for easy programming of all stimulation,
202 measurement, and feedback parameters within each of the individual 96 wells (**Figure 2B**). The GUI home
203 screen features three functions: 1) "Calibrate OD", 2) "Calibrate Blue", and 3) "Start Experiment". The
204 calibration buttons allow for automated calibration of the oPR components (see next section). After calibration,
205 the "Start Experiment" button leads to a window titled "Stimulation Protocol", which prompts the user to define
206 optogenetic stimulation protocols and to assign those protocols to individual wells or groups of wells. For each
207 protocol, the user can specify the intensity of the blue LED, the duration that the LED will be ON, and the
208 subsequent duration that LED will be OFF. The LED will loop through these ON and OFF durations
209 continuously. Up to 96 distinct protocols can be specified. The user can also specify a feedback function to be
210 applied to each pattern of wells. Arbitrary feedback inputs, outputs, and algorithms can be programmed in the
211 FeedbackFuncs.py file (see **design files** and **manual**). In the subsequent window, the user defines
212 measurement parameters for the optoReader, specifically the duration and frequency of OD and fluorescence
213 readings. The same measurement parameters are applied to all wells. For each type of measurement, the user
214 can specify the number of individual readings that will be averaged in order to minimize measurement noise.
215 For the studies in this report, we averaged 100 readings per measurement. In the final window, the GUI allows
216 the user to review and edit the experimental protocols before running the experiment. At the start of the
217 experiment, the software generates .csv files in which the OD and fluorescence measurements will be
218 recorded and updated. At the end of the experiment, the user retrieves these .csv files and processes them as
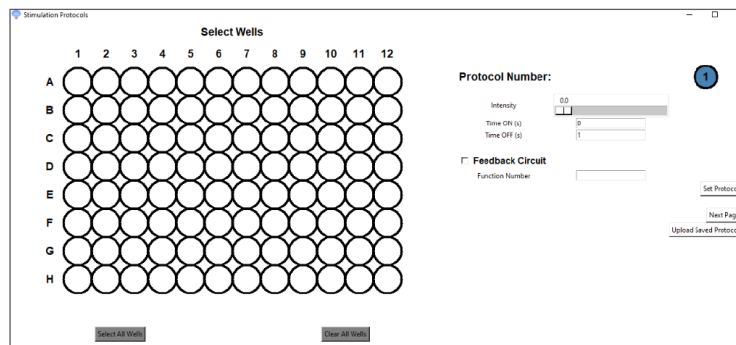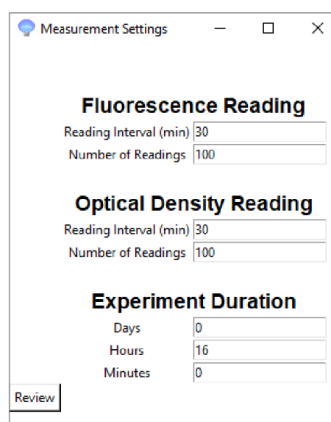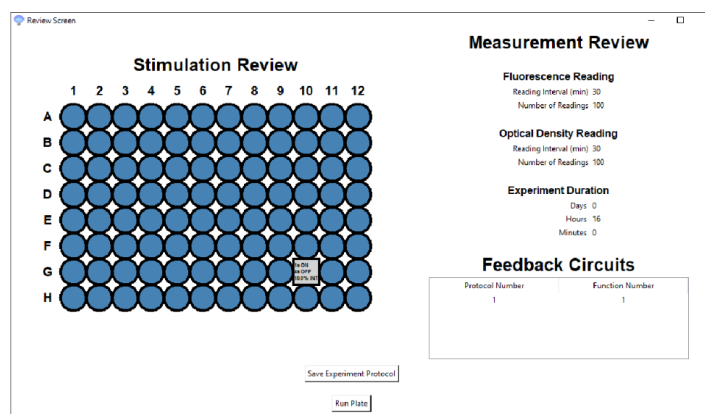219 needed for data analysis and visualization.
220
221
222
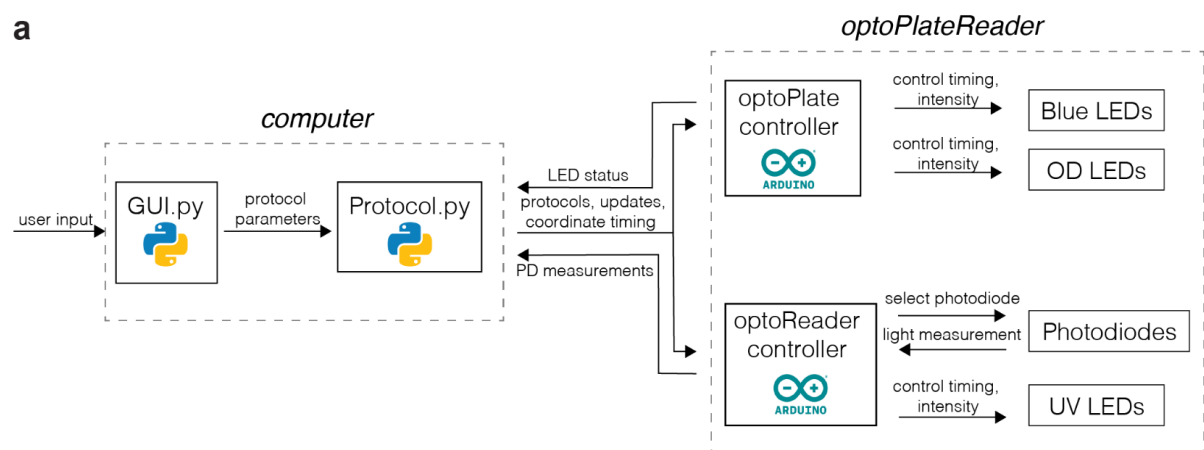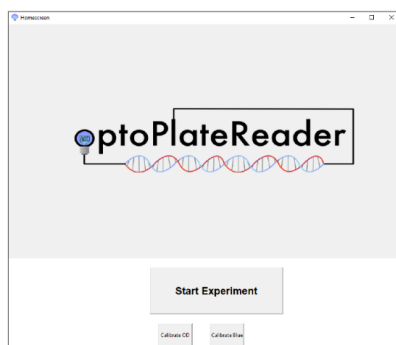
Figure 2. oPR software workflow and graphical user interface (GUI) for programming oPR protocols. a Software architecture for communication between user, computer, and oPR. The GUI and Protocol python scripts send user-defined stimulation and measurement protocols to the optoPlate and optoReader Arduinos that control individual components in both device modules. Photodiode measurements collected by the optoReader Arduino are returned to the computer for reporting or feedback-driven signal adjustments. **b** Windows of the GUI. (1) The user can automatically calibrate OD and Blue LEDs from the homescreen. (2) Wells, light dose, illumination timing, and feedback algorithm are specified for up to 96 independent protocols. (3) Photodiode reading frequency parameters are specified. (4) The user can review and save their experimental protocols prior to running the experiment.

233
234

235 *Calibrating the optoPlateReader*
236 Each of the four optical elements of the oPR (UV LED, blue LED, OD LED, photodiode) must be calibrated to
237 minimize measurement noise that originates from variability during component manufacture or device
238 assembly (**Figure 3**). Each set of components can be calibrated in an automated manner using the GUI (OD
239 and Blue LEDs) or in a semi-automated manner using files available in the **oPR Repository** (See **Methods**)
240 (UV LEDs and Photodiodes). Calibration involves measuring each of the 96 components, calculating their
241 variability (coefficient of variation (CV), the standard deviation normalized by the mean), calculating
242 normalization factors to minimize CV, performing new measurements with the normalization factors, and
243 iterating over multiple rounds until CV is minimized. We reasoned that, because each well contains a light
244 detector (the photodiode), we could first calibrate the photodiodes to an external, uniform light source and then
245 subsequently calibrate each LED using the calibrated photodiodes. A detailed description of all calibration
246 procedures can be found in the **Methods** section.
247

248 To calibrate the photodiodes, we used an instrument that projected white LED light uniformly over a surface,
249 and we further used diffuser film to homogenize illumination and adjust irradiance intensity, which we
250 confirmed with a handheld power meter (see **Methods**) (**Figure 3A**)**.** Uncalibrated optoReader photodiodes
251 initially recorded 96 values with CV = 5.1%. After one round of calibration, we measured dramatically less
252 variation between photodiodes (CV = 1.0%). Further calibration rounds yielded no further decrease in CV.
253 Calibration factors were also found to be independent of light exposure intensity (**Supplementary Figure 3**).
254

255 We then used the calibrated photodiodes to calibrate the blue, OD, and UV LEDs in the fully assembled oPR.
256 Blue LED variability (CV = 15.9%) was reduced to 2.8% after two rounds of calibration (**Figure 3B**). The OD
257 LEDs were calibrated in a similar manner except that LB was added to the wells to reproduce the light
258 refraction caused by liquid in the wells, which we hypothesize could contribute to well-to-well variation in OD
259 readings. After 3 rounds of calibration, OD LED variability was reduced from CV = 16.6% to 0.5% (**Figure 3C**).
260 Finally, we calibrated the UV LEDs by measuring variability in fluorescence emission of Lucifer Yellow dye that
261 was added to each well of a sample plate. Lucifer Yellow dye has similar fluorescence spectra to mAmetrine
262 and thus is compatible with the optical configuration of the oPR. After 2 rounds of calibration, measurement
263 variability decreased from CV = 9.8% to 1.0% (**Figure 3D**).
264

265 We note that the OD LED calibration should be performed at the beginning of each experiment since we have
266 found significant variability in OD readings between experiments, likely due to slightly different sample
267 refractive properties and device alignments. OD LED calibration is performed using the "Calibrate OD" function
268 on the opening window of the GUI (**Figure 2B**). By contrast, calibration of the LEDs can be performed much
269 less frequently, primarily to account for changes in LED brightness due to extended use. Calibration factors
270 were robust to changes in temperature, allowing accurate readings to be taken at 37°C based on calibration
271 factors obtained at room temperature (**Supplementary Figure 4**).

272


273
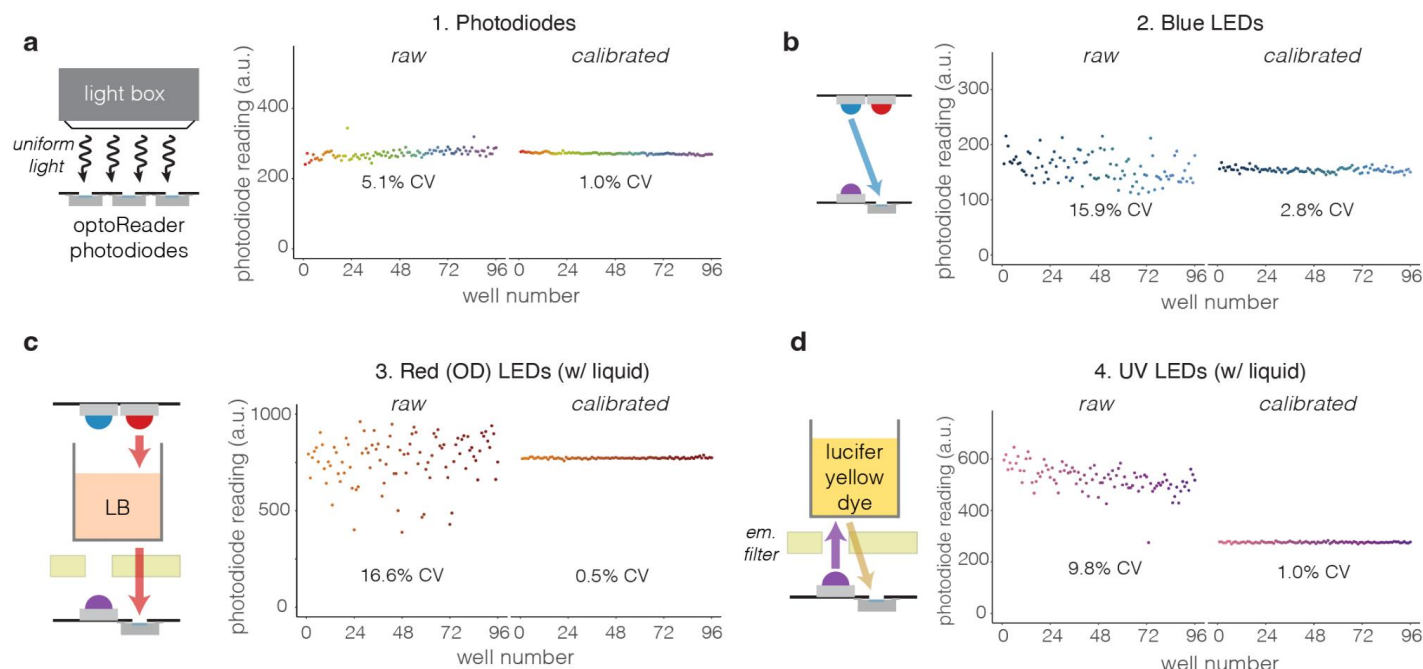
Figure 3. Component calibration for precise stimulation and measurement between wells. **a** Calibration of photodiodes must be performed first in order to use photodiodes to calibrate the LED components. Photodiodes are calibrated by using a uniform white light source to illuminate all wells with the same light intensity. **b** Blue LEDs are calibrated with the photodiodes in a fully assembled oPR, using an empty 96-well plate and no emission filter. **c** OD LEDs are calibrated in a fully-assembled oPR with an equal volume of LB in each well to to account for light refraction through the medium. This calibration should be performed at the start of each experiment using the "Calibrate OD" function found in the GUI. **d** UV LED calibration is performed in a fully-assembled oPR with an equal volume of diluted lucifer yellow dye in each well (40 µg/mL shown here). Calibration is performed by adjusting LED intensity to normalize variation in the measured emission intensity of the dye. In all cases, calibration reduced variation between wells to CV = 1-3%

284

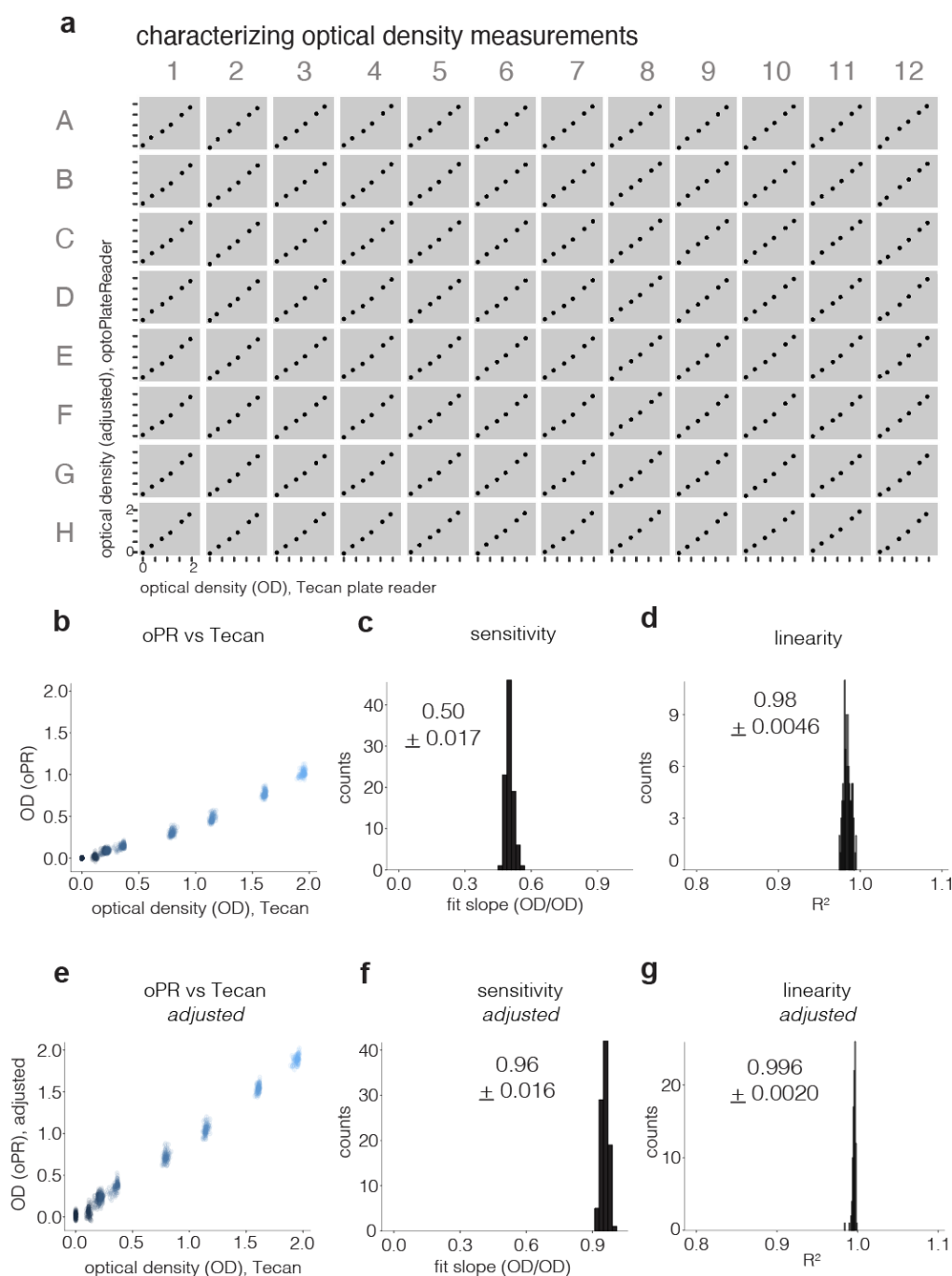285   *Characterizing oPR measurements.*
286   With a fully calibrated oPR, we sought to characterize the limits and sensitivity of fluorescence signal detection.
287   We generated a dilution series of Lucifer Yellow dye (2-250 µg/mL), and we measured each concentration in
288   every well of a 96-well plate (**Figure 4, Supplementary Figure 5**). Fluorescence readings were highly
289   consistent between the 96 wells. Readings increased monotonically with concentration, with a linear region
290   extending to 40 µg/mL (**Figure 4A**). The average lower limit of detection (LOD) (1.0 +/- 0.2 µg/mL) was also
291   highly consistent between wells (**Figure 4B**), yielding an average dynamic range of 40 (**Figure 4B**).
292   Measurement sensitivity — or, the relationship between the photodiode counts and concentration — showed
293   little variation between wells (12.5 +/- 0.3 counts/µg/mL, **Figure 4C**) and was highly linear (R^2 = 0.996 +/-
294   0.002, **Figure 4D**). Collectively, these results demonstrate that the oPR can measure fluorescence in 96 wells
295   simultaneously with high sensitivity, high precision, and low variance between wells. Of note, although the oPR
296   was not as sensitive for fluorescence measurements as could be obtained by a commercial plate reader (LOD
297   of Tecan Infinite M200 Pro: 12 +/- 0.3 ng/mL (**Supplementary Figure 6**)), the oPR was sufficiently sensitive for
298   robust fluorescence measurements from bacterial cultures (see **Figures 6-8**).
299
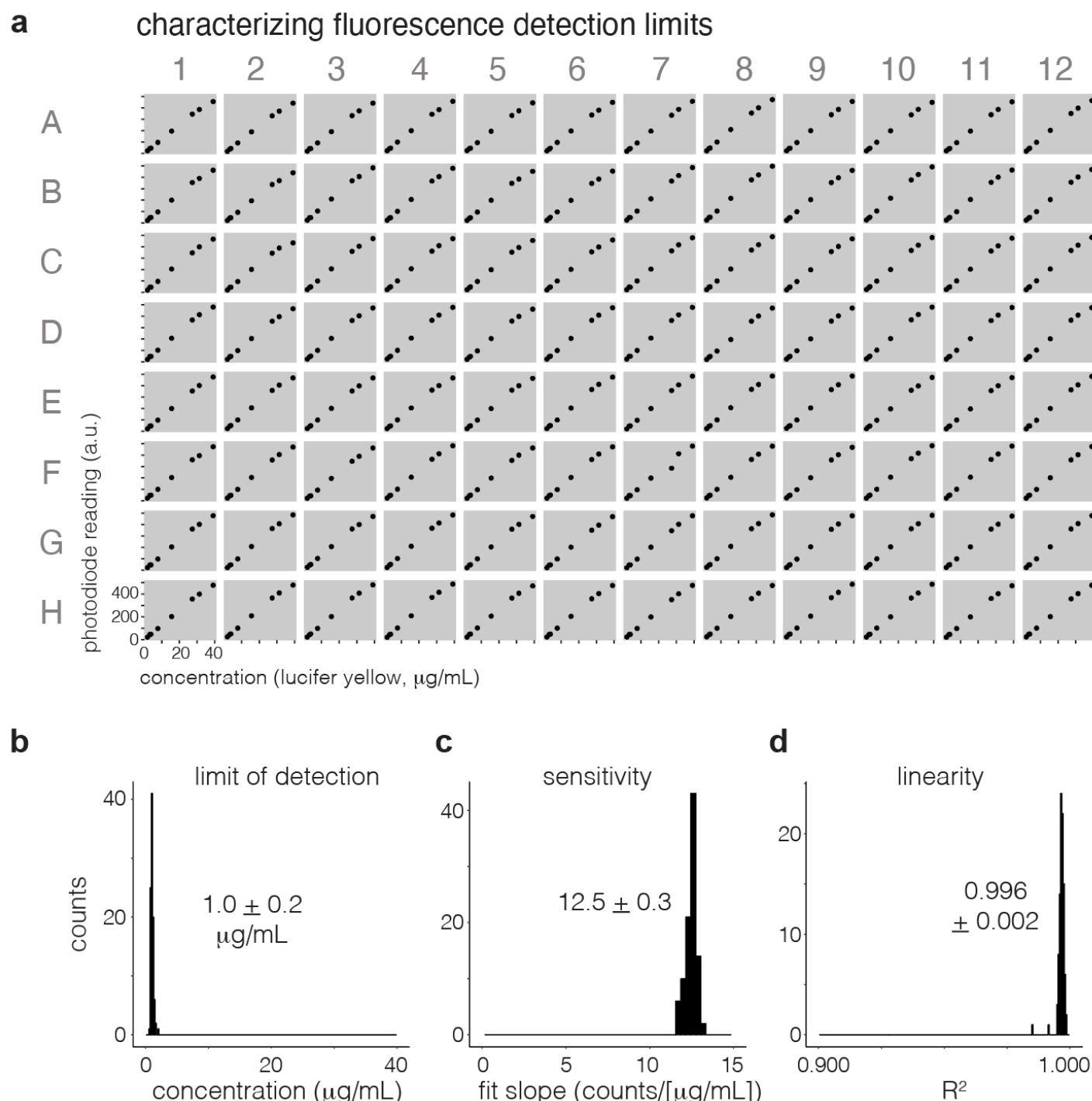
Figure 4. Characterization of fluorescence detection. a Fluorescence measurements of lucifer yellow dye were taken over a range of concentrations in each of 96 wells in a calibrated oPR. The linear range of measurements is shown (full concentration range in **Supplementary Figure 5**). **b** The average limit of detection of each well was 1.0 +/- 0.2 µg/mL, showing low variability between each of the 96 wells. **c** The sensitivity —or, the slope of the linear fit of the relationship between photodiode counts and concentration — also showed low variability between wells. **d** R^2 values of the fits described in **(c)** confirm linearity in all wells.

307

308   We next characterized the optical density measurement capabilities of the oPR by comparing oPR

309   measurements to those obtained with a Tecan Infinite M200 Pro. We generated a twenty-fold dilution series of

310   1.1 μm polystyrene beads, a common reagent for OD measurement calibrations[21]. We plated each dilution into

311   all wells of a 96-well plate and measured optical density in both the oPR and the Tecan in rapid succession.

312   OD measurements from the oPR vs the Tecan measurements showed a highly linear relationship in all wells

313   (R^2 = 0.98 $\pm$ 0.004, **Figure 5A-D**. For details on OD calculation, see **Methods**).

314

315   Despite the linear relationship, the magnitude of the oPR reading was approximately 1/2 of the Tecan reading

316   (**Figure 5C**). Because Tecan readings are often used as a standard for OD readings, we derived a

317   transformation for each well that adjusted oPR OD readings to reflect those of the Tecan (see **Methods** for full

318   details). The equation for each well was then applied to oPR readings taken during a subsequent calibration

319   experiment to generate "Adjusted oPR readings" which matched the amplitude of OD readings of the Tecan

320   (**Figure 5E-G**). Importantly, oPR readings were consistent between separate experiments, meaning that one

321   calibration experiment can be used to calculate adjustments that can then be applied to future oPR

322   experiments. For a comparison between Tecan and oPR CVs at each OD, see **Supplementary Figure 7.**

323

Figure 5. Characterization of optical density measurements. a oPR OD measurements were characterized by making dilutions of 1.1 μm diameter plastic beads, plating these dilutions in each well of a 96-well plate, and measuring OD on the oPR and on a Tecan Infinite M200 in rapid succession. Each Tecan reading is the average of 25 readings from the center of each well. Data shows calibrated/adjusted results, as described in **Methods**. **b** Raw data from (**a**) is overlaid. Each color represents a distinct dilution of beads. Each cloud has 96 data points representing each of 96 wells. **c** A histogram of the slope of linear fits of each plot in part (**a**)**.** Average sensitivity is mean slope +/- 1 s.d. of 96 fits. **d** A histogram of R^2 values of linear fits from (**b**). Average R^2 is mean +/- 1 s.d. of 96 fits. **e** To allow direct comparison between Tecan readings and oPR, a transform function was calculated from data shown in **b-d** for each well. This transform was then applied to a second independent data set to generate "adjusted oPR readings" that closely matched Tecan readings. **f** Slopes of these adjusted data show high correspondence (slope ~1) and high linearity (**g**) between oPR and Tecan OD readings.

337
338 *Using the oPR to stimulate and measure bacterial transcription and growth.*
339 To test the oPR's ability to read bacterial growth and mAmetrine fluorescence, we generated *E. coli* that
340 express mAmetrine under an arabinose-inducible promoter (**Figure 6A)**. We inoculated LB with these bacteria,
341 plated in each well of a 96-well plate, and measured bacterial fluorescence and OD in the presence or absence
342 of arabinose over 18 hrs in a 37 °C incubator. All live cell experiments were performed with 45 µL of parrafin oil
343 deposited over 125 µL of culture samples. Paraffin oil prevented evaporation from the wells while permitting
344 gas exchange and normal cell growth, consistent with previous work[22] (**Supplementary Figure 8**). In all wells
345 that received arabinose, the oPR detected mAmetrine fluorescence within the first two hours of arabinose
346 addition, increasing and then plateauing throughout the experiment (**Figure 6B).** No fluorescence change was
347 detected in the absence of arabinose. Optical density similarly increased and then plateaued in each well
348 throughout the experiment (**Figure 6C**). In sum, these data demonstrate that the oPR can sensitively read
349 fluorescence and absorbance over physiologically relevant regimes in bacterial culture, with low variability
350 between wells. Moreover, these results show that the oPR is compatible with operation in bacterial incubators
351 held at 37 °C and while shaking at 1000 RPM. Shaking dramatically enhanced growth of the bacterial cultures
352 (**Supplementary Figure 9**).
353
354
355
356
357
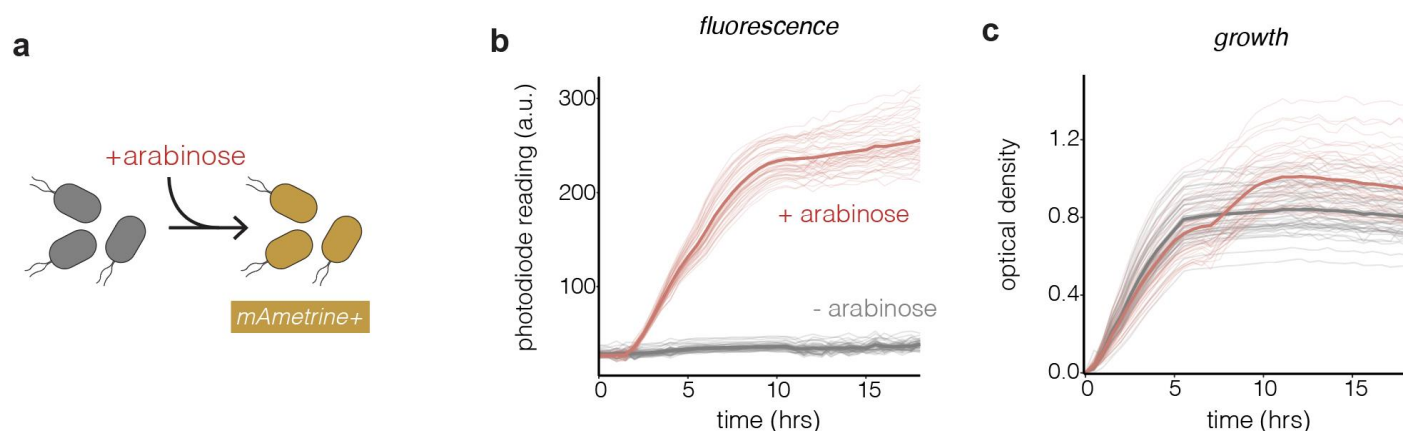
358
359 **Figure 6. The oPR detects fluorescence and bacterial growth in real time**. **a** The oPR was used to
360 measure growth and fluorescence in *E. coli* that expressed mAmetrine under an arabinose-inducible promoter.
361 **b** mAmetrine fluorescence was detected in every well that was treated with arabinose (red), and was not
362 detected in the absence of arabinose (grey). Each trace corresponds to readings from an individual well. Bold
363 traces represent means of all 48 replicates per condition. Fluorescence was measured every 20 min for 18 hrs.
364 **c** OD readings of the same wells depicted in (**b**). Both measurements were taken every 20 min at 37 °C. Each
365 trace corresponds to readings from an individual well. Bold traces represent means of all 48 replicates per
366 condition. The increase in OD at ~7 hours in the "+arabinose" wells is likely due to the bacteria switching to
367 arabinose as a carbon source once glucose is exhausted[23].
368
369

370 Although the oPR optical configurations are optimized for mAmetrine, we also tested whether the device could
371 be adapted to measure other fluorophores. By replacing the UV excitation LED with a blue LED (475 nm), the
372 oPR could measure GFP expression in *E. coli* cultures (**Supplementary Figure 10)**. However, GFP, which
373 was driven by the same promoter as mAmetrine in previous experiments, gave fluorescence signals that were
374 ~30% as strong as mAmetrine. This is likely because our emission filter more strongly attenuates GFP
375 emission (507 nm) relative to mAmetrine emission (526 nm) (**Figure 1B**). Nevertheless, this experiment
376 demonstrates that the oPR can be applied to detect fluorophores besides mAmetrine with appropriate changes
377 to the LEDs and/or emission filters.
378
379 Next, we tested the oPR's ability to optogenetically stimulate cells. We transformed cells with one of two
380 plasmids — pDawn or pDusk[24]— that placed mAmetrine under blue light inducible transcriptional control. In
381 pDawn, blue light stimulates reporter transcription that turns off in the dark, whereas in pDusk, blue light
382 represses transcription that is otherwise constitutively active in the dark (**Figure 7A,B**). We seeded both
383 strains in a single 96-well plate (48 wells for each strain). We then programmed the oPR to stimulate 24 wells
384 of pDawn strain with blue light (pulsed with 3 seconds ON, 7 seconds OFF), while the remaining 24 wells each
385 received no light. For the pDusk strain, the oPR was programmed to keep 24 wells in the dark while stimulating
386 the remaining 24 wells in the same manner as for pDawn. Fluorescence and OD were measured every 30
387 minutes. The oPR successfully measured increasing mAmetrine fluorescence in all illuminated pDawn wells
388 and dark pDusk wells over 10 hours of culture (**Figure 7C,D,** blue traces). Conversely, no fluorescence was
389 detected in any dark pDawn well or illuminated pDusk well (grey traces), indicating that the oPR successfully
390 confined optogenetic stimulation to only the desired wells. OD measurements successfully captured growth
391 dynamics of both strains (**Figure 6C**). These data also demonstrate that UV light can be used to measure
392 fluorescence without triggering a blue-light sensitive optogenetic tool, likely due to sparse illumination by the
393 UV LED.
394
395
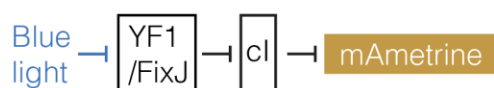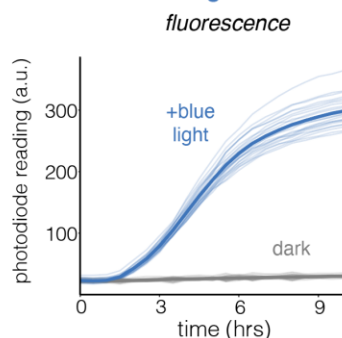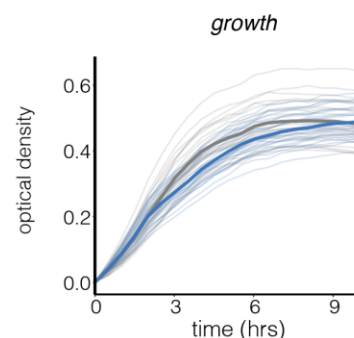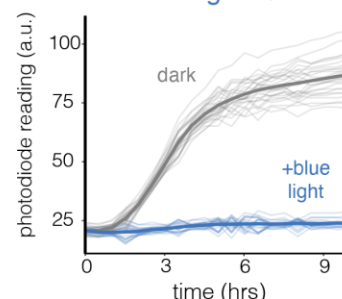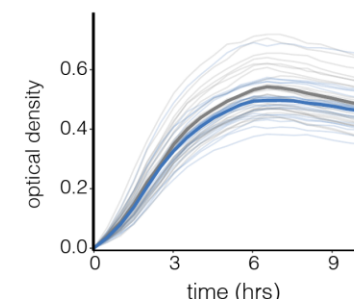
Figure 7. Simultaneous optogenetic stimulation and spectroscopy in growing bacteria.
The oPR was used to stimulate and measure *E. coli* that expressed mAmetrine controlled by one of two optogenetically-controlled transcriptional circuits, pDawn (**a**) and pDusk (**b**). In pDawn, blue light triggers mAmetrine expression, while in pDusk, blue light suppresses its constitutive expression. Fluorescence (**c**) and OD (**d**) of pDawn samples in response to blue light (blue) and dark (grey) conditions. The oPR detects mAmetrine only in samples exposed to blue light, demonstrating successful optogenetic induction. Traces represent measurements from individual wells, and bold traces represent means from each condition (24 replicates with blue light, 24 replicates in the dark). Data was collected every 30 minutes for 10 hrs at 37 °C. Fluorescence (**e**) and OD (**f**) of pDusk samples in response to blue light (blue) and dark (grey) conditions. The oPR detects mAmetrine only in samples that were not exposed to blue light, demonstrating successful optogenetic suppression. Traces represent measurements from individual wells, and bold traces represent means from each condition (24 replicates in the dark, 24 replicates with blue light). Data was collected every 30 minutes for 10 hrs at 37 °C.

411   *All-optical feedback control in 96 independently-controlled experiments*
412   The ability to simultaneously stimulate and measure cells allows for all-optical feedback control in 96
413   independent parallel experiments. To test this ability, we performed 96 experiments representing three classes
414   of experiments that tested the main control knobs that could be implemented in custom feedback-controlled
415   experiments (**Figure 8A**). The three classes of experiment were 1) constant open-loop blue light exposure with
416   varying light intensities, 2) fluorescence-based feedback where optogenetic stimulation was halted once a
417   particular mAmetrine fluorescence value was reached, and 3) OD-based feedback where optogenetic
418   stimulation would only be applied after the culture reached a certain OD. For each class of experiment, we
419   tested 8 distinct feedback parameters, and each parameter set was performed in biological quadruplicate, all
420   on one microwell plate For experiments in class 1, we achieved graded expression mAmetrine between 0.5%
421   and 10% of maximum blue light intensity (**Figure 8B**). For experiments in class 2, mAmetrine expression was
422   successfully halted after fluorescence reached the designated level, with a small time lag due to inactivation
423   kinetics of the transcriptional cassette, during which fluorescence continued to increase slightly before reaching
424   a plateau (**Figure 8C**). For experiments in class 3, cultures triggered at higher ODs showed delayed
425   mAmetrine expression and lower total levels of mAmetrine relative to cultures triggered at lower ODs (**Figure
426   8D-F**). These three experimental classes represent foundational operations that can be combined for more
427   complex, custom feedback applications. Such custom functions can be written in the *FeedbackFuncs.py* file
428   and can implement any mathematical process available in Python. Importantly, because of low well-to-well
429   variability of stimulation and measurement in the calibrated oPR, 96 independent feedback-controlled
430   experiments can be performed with low resultant variability between wells (**Figure 8B-D**).
431
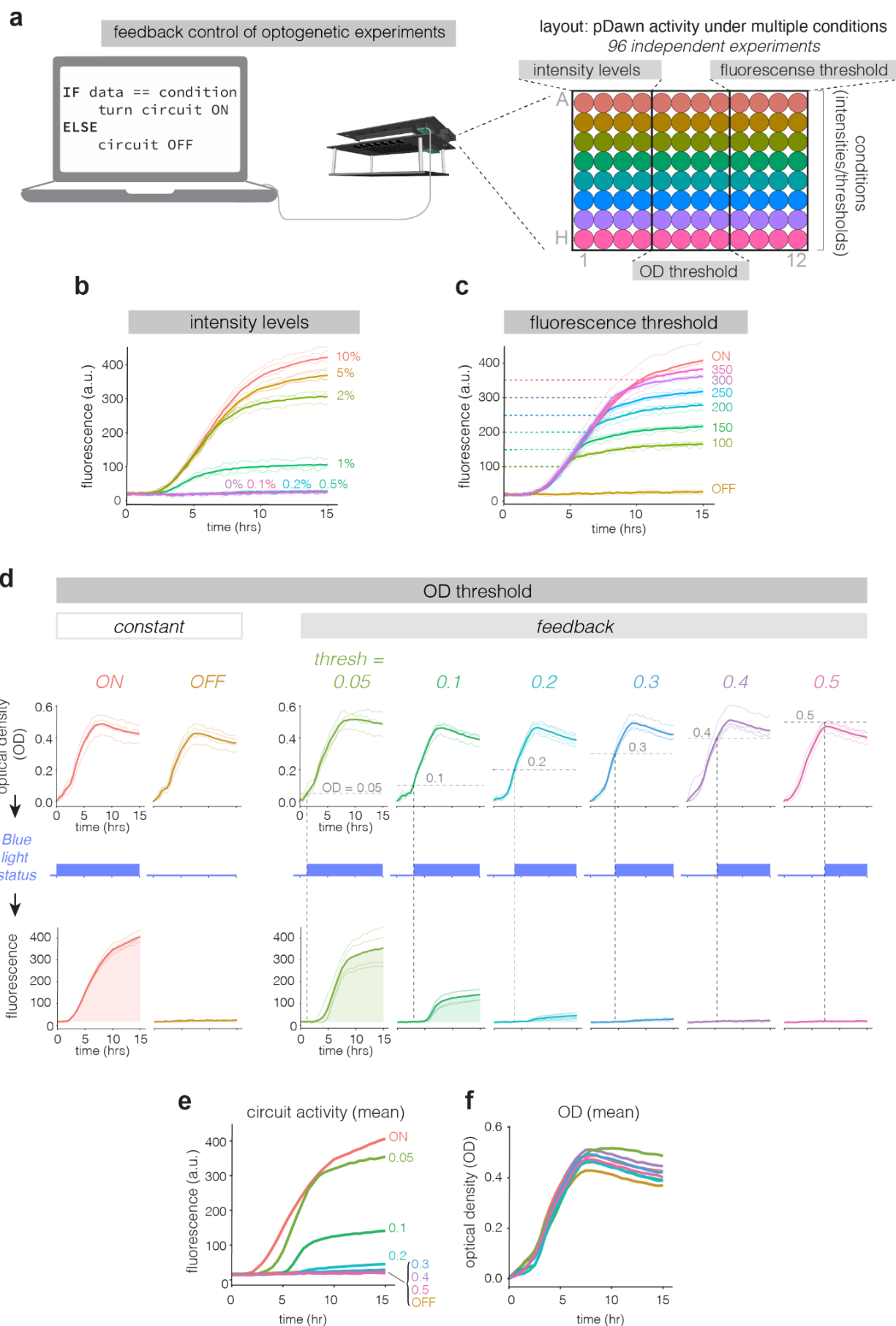
Figure 8. oPR allows computer-in-the-loop feedback control of bacterial behavior. a Diagram of "computer in the loop" feedback control of bacterial cultures, performed in 96 independently-controlled feedback experiments. The plate was divided into classes of experiments: constant light at different intensity levels, an fluorescence threshold at which blue light exposure is turned on, and an OD threshold at which blue light exposure is turned off. Each color of well represents a variation of a parameter within each feedback experimental class. **b** mAmetrine expression from bacteria stimulated with different light intensities. Each trace represents a single well at the corresponding blue light intensity. **c** mAmetrine expression in bacteria whose expression was halted once their fluorescence reached a predefined threshold. Dashed lines indicate the threshold for each trace. **d** OD (top row) and mAmetrine fluorescence (bottom row) in bacteria whose mAmetrine was optogenetically stimulated once their OD reached a pre-defined threshold. Dashed lines indicate the OD threshold. Mean fluorescence (**e**) and OD (**f**) are overlaid for clearer comparison of performance of each condition from (**d**). For (**b-d**), each light trace represents a single well that was controlled based on its own state. bold traces represent the average of the four replicate wells per condition.

Discussion

The optoPlateReader (oPR) is a device for fully programmable optogenetic experiments, where stimulation, spectroscopic measurements, and feedback adjustments occur in an automated, pre-programmed manner, in 96-well plates. Because there are no moving parts and no wires other than power cables and USB cables, the oPR is robust to mechanical perturbations, allowing it to be used on shakers and within incubators. We showed that the oPR can read fluorescence and OD from bacteria with high sensitivity and low variability between the 96 well positions. The high precision measurements allowed direct comparison of different wells in the same plate, and further enabled computer-in-the-loop feedback control, where the optogenetic stimulus of each well can be dynamically updated based on its current state. We also developed software that integrates and controls all components of this device, including a graphical user interface that allows easy programming of complex optical reading, writing, and feedback parameters for each individual well. Importantly, the oPR is an open source device that can be built with no prior expertise in electronics within ~6 hours, at low cost, and can be readily modified for custom applications.

We overcame two main obstacles in our hardware design. The first was in optimizing the optical components and their orientation to allow sensitive OD600 and fluorescence measurements. In particular, the compact placement of the photodiode and the adjacent UV LED could lead to contamination of the fluorescent signal with the excitation light. We overcame this challenge in three ways. First, we used a photodiode that was mounted on the opposing side of the PCB and faced the sample through an aperture. Second, we selected a photodiode with a low responsivity in the UV range, providing a measure of filtration of the UV LED light. Finally, we included a plastic emission filter film that further blocked light in the UV range but passed light between 470 nm and 650 nm, permitting OD600 measurements and mAmetrine emission detection. These optimizations were enabled by selection of the long-Stokes-shift fluorescent protein mAmetrine, which provides sufficient separation in the excitation and emission spectra to allow effective filtration of excitation light with inexpensive filters while minimally affecting fluorescence or OD detection. A second important design challenge was in the variability among the three LEDs and one photodiode. After device assembly, we measured up to ~20% variability between the 96 components of each type. Such variability could further compound, for example if UV LEDs with high variance are used to stimulate fluorescence that is measured by photodiodes with high variance. Such measurements would have high uncertainty, challenging interpretation and making comparisons of values from different wells impossible. We overcame this limitation by 1) designing 3D adapters for optimal and consistent alignment between oPR components, and 2) developing careful calibration protocols, first for the photodiodes, and then using the calibrated photodiodes to calibrate remaining LEDs. These measures were essential to obtaining the tight correspondence of fluorescence values between wells of the same conditions, and for the robust OD measurements that enabled precise OD-based feedback control. If further reduction of technical variability is required, readings from replicate wells can be averaged together during the experiment via the "grouping function" found in the GUI (See **oPR Repository Usage Manual**).

The ability to perform 96 parallel feedback experiments represents the biggest advance enabled by the oPR. Such control could be highly advantageous for fields like metabolic engineering, where optogenetic transcriptional control can dynamically optimize flux through engineered metabolic pathways[25]. Although the parameter space for such optimizations is vast (spanning different intensities, waveforms, duty cycles, durations, etc), the ability to automate ~100 such experiments simultaneously and without user intervention during the experiment allows dramatically faster sampling of these parameters. Furthermore, feedback control algorithms could allow the oPR to optimize stimulation protocols on the fly, outputting the stimulation parameters it used to achieve the predefined target state. Moreover, because of the small footprint and low cost of the oPR, multiple devices could be operated in parallel, further increasing throughput.

Although we characterized the oPR for measuring growth, fluorescence, and for optogenetic stimulation of bacterial cultures, the device and its submodules could be applied more broadly. Similar experiments could

495 be performed for example in yeast, mammalian cells, or even cell-free systems, though the electrical circuitry
496 that sets the sensitivity and dynamic range would likely have to be optimized for each application separately. In
497 addition, the optoReader module could be used as a standalone device, similar to an existing 96-well
498 phototransistor array that measured absorbance[19], but with the added capability of fluorescence
499 measurements. Alternatively, a well-calibrated optoReader could be used to rapidly calibrate the optoPlate-96
500 or other LED arrays used for optogenetics, which have a typical variation of 10-20% in intensity between LEDs
501 after assembly[2,27,28] and thus require calibration for precise greyscale optogenetic control.
502   Several future improvements could further empower experiments with the oPR. Optimization for
503 fluorescent proteins other than mAmetrine, or even to allow reading of multiple fluorescent proteins, would
504 expand experimental capabilities. Such modifications should be feasible with high-quality emission filters like
505 those found on fluorescence microscopes, though at increased cost. The oPR also has exposed circuitry which
506 has the potential to become corroded, for example as a result of accidental spills of culture media. Thus a
507 physical barrier to protect the circuitry would increase its robustness, though we note that no spillage or loss of
508 functionality was observed despite shaking during all live-cell experiments. In addition, the oPR circuitry could
509 be enhanced to allow wireless communication with the computer, and also to increase sensitivity and dynamic
510 range of light detection.
511   In sum, the oPR is device for high-throughput, feedback-enabled optical reading and writing in cells,
512 and it achieves such sophisticated experiments in a compact, inexpensive, and open-source manner, opening
513 new horizons for optogenetic and cybernetic interfaces with biological systems.
514
515

525

Author Contributions:
526
527 W.B., D.G.M., J.L.A, B.Y.C.,L.J.B conceived study. S.D., W.B., D.G.M, G.L., J.H., G.Q., G.L., L.S., G.H., S.M.,
528 M.S.M., M.P., S.M., J.L.A., B.Y.C., L.J.B. designed hardware structure and component layout. S.D., W.B.,
529 D.G.M, G.L., J.H., G.Q., G.L., L.S., G.H., S.M., L.J.B. constructed hardware, performed experiments, and
530 analyzed data. S.D., G.L., J.H., W.B., D.G.M, developed software. S.G.M., J.L.A., B.Y.C., L.J.B. supervised
531 and advised work. S.D., W.B., L.J.B. drafted manuscript and figures. All authors contributed to editing.
532
533
534

Supplementary Figures
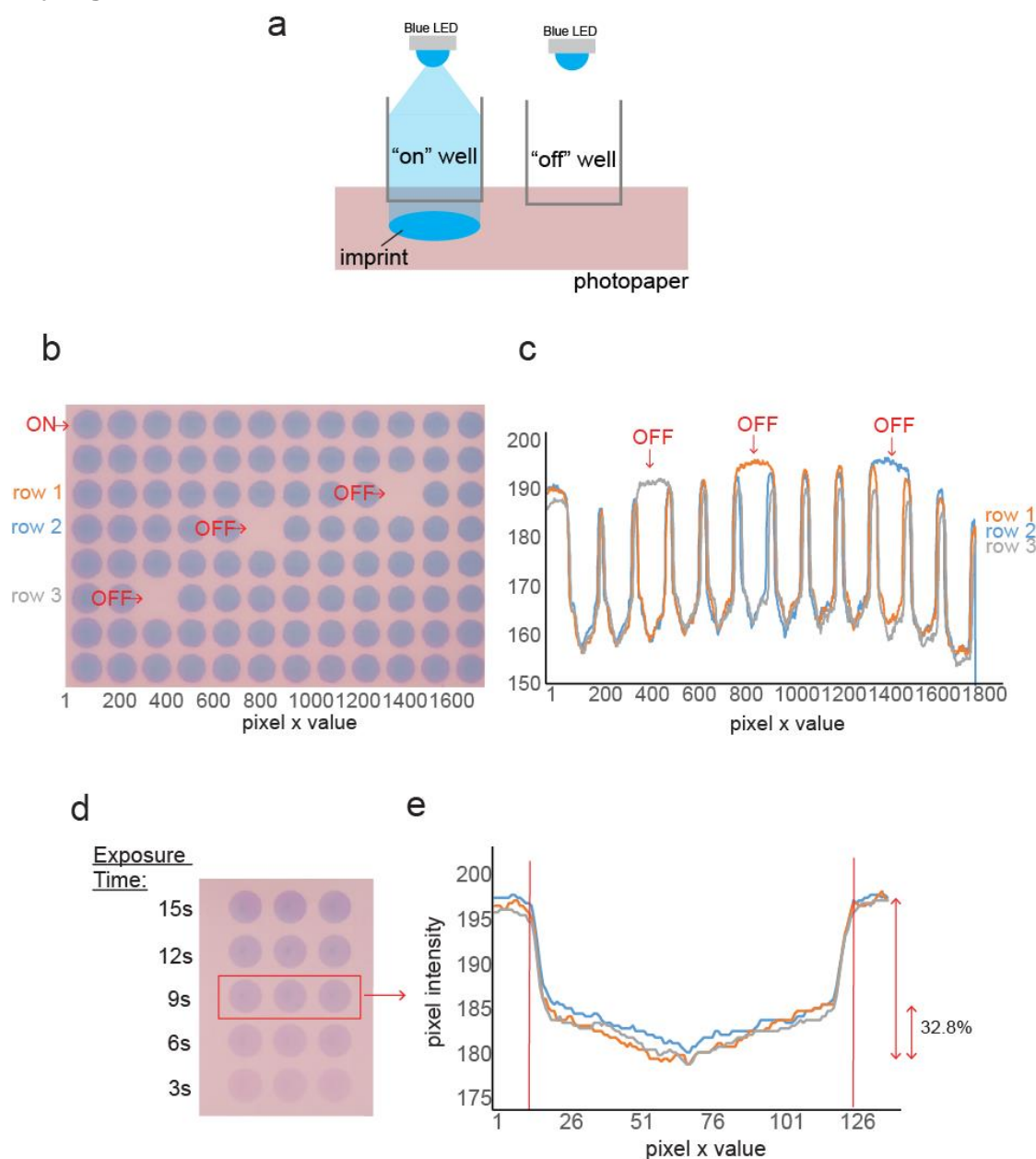
Supplementary Figure 1. Insulation of light between wells and homogeneity within wells. a Photopaper allows for imprinting and recording of light exposure underneath a 96 well plate from the blue LEDs[9]. **b** All wells of the optoPlate's blue LEDs were set to maximum except the 3 indicated as "OFF." The optoPlate was mounted on a 96 well plate with photopaper placed below the plate. No imprint was observed in OFF wells, despite all surrounding wells being set to maximum intensity for 5 minutes. This indicates that light spread between wells is negligible. **c** Quantification of the intensity across each row of wells of the exposed photopaper in **(b)** shows that OFF wells do not display detectable imprints from light exposure despite neighboring wells being set to maximum intensity. Data represents a line profile of the pixel intensity across the center of each row of wells. **d** Photopaper can also be used to analyze light uniformity within wells. Triplicate wells were exposed to blue light for varying times in order to find a non-saturating exposure time. 9s was chosen for quantification. **e** Line profile of the pixel intensities across the center of each well from the 9s exposure condition from **(d)**. Blue light intensity varies by 32.8% from the center to the edge of the wells (indicated with red lines). However, this non-uniformity is can be overcome either by 1) stimulating with strong blue light such that even the weaker light at the periphery is saturating for the optogenetic protein, or 2) shaking the cultures during growth, homogenizing the effective light intensity that the bacteria experience over time.

553
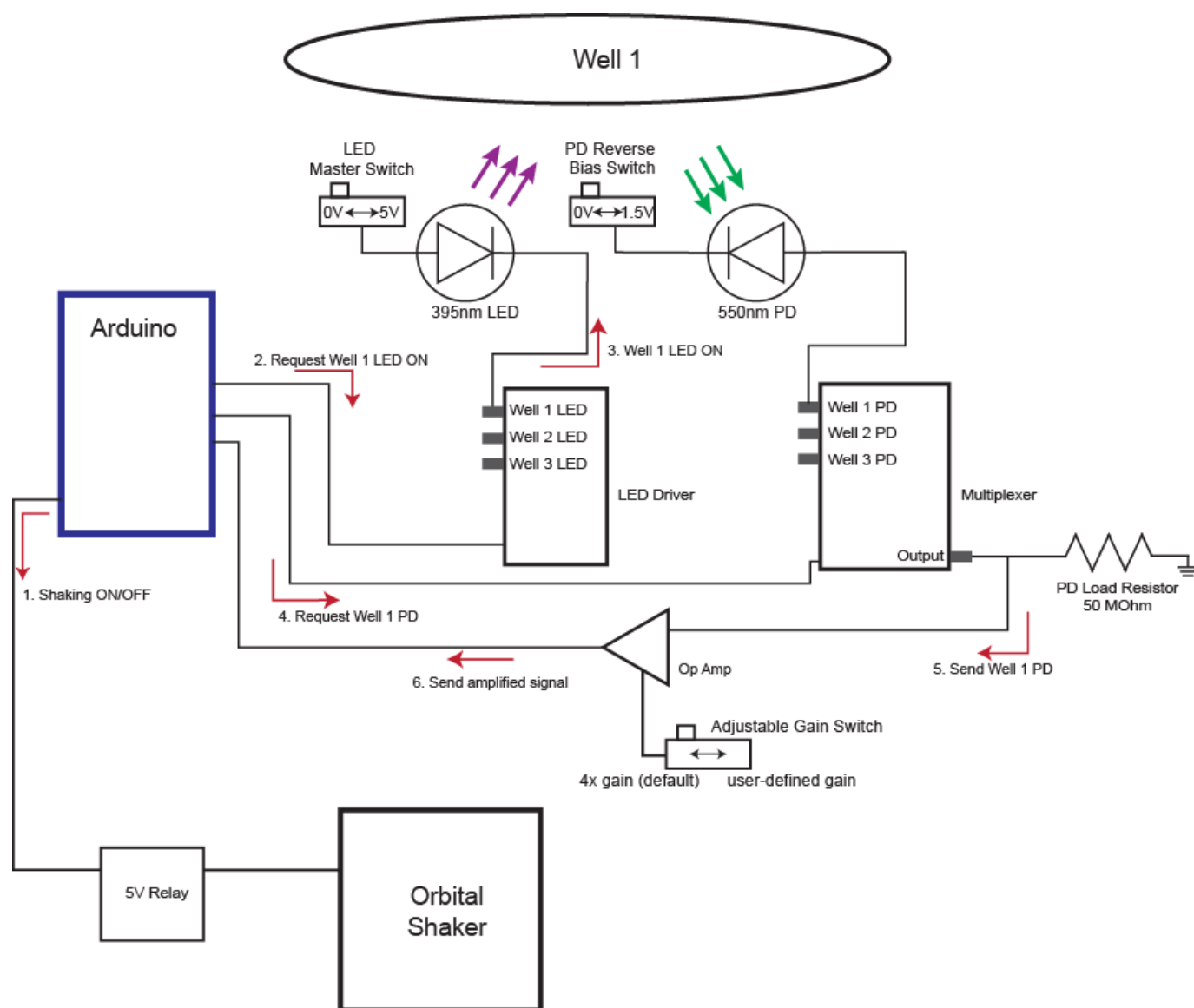
554
555
Supplementary Figure 2. oPR circuit diagram for fluorescence readings in a well. To acquire fluorescence readings for a well, the following sequence of events occurs: 1) Shaking is paused during measurements. 2) The oPR Arduino sends a signal to the LED drivers requesting that the UV LED for that well be switched on; 3) The LED driver switches on the LED for that well while leaving all other LEDs off. The LED 5V switch must be set to the 5V position for LEDs to turn on. This switch ensures that the LEDS are only operational when desired to prevent inadvertent illumination on samples or investigators. 4) The Arduino then sends a command to the multiplexer to select the photodiode (PD) for that well. The PD signal can be altered by changing the Reverse Bias switch. 0V (used in this study) allows detection of lower intensity signals by reducing the background signal produced by the photodiodes. 1.5V allows for detection of higher intensity signals by raising the point of signal saturation. This is because a greater maximum voltage can be produced by the photodiode than is possible without a reverse bias. However, this also causes a higher background signal when no fluorescence is present. 5) The signal from the PD is then sent to an amplifier that multiplies the signal by an adjustable gain. The Adjustable Gain switch can be set to 4x (used in this study) or a user defined gain (by adding a resistor of a desired value as labeled in the component diagram). 6) The final signal is sent to the Arduino for processing. A similar sequence of events takes place for OD readings, with additional communication with the optoPlate to coordinate illumination of the OD LED.
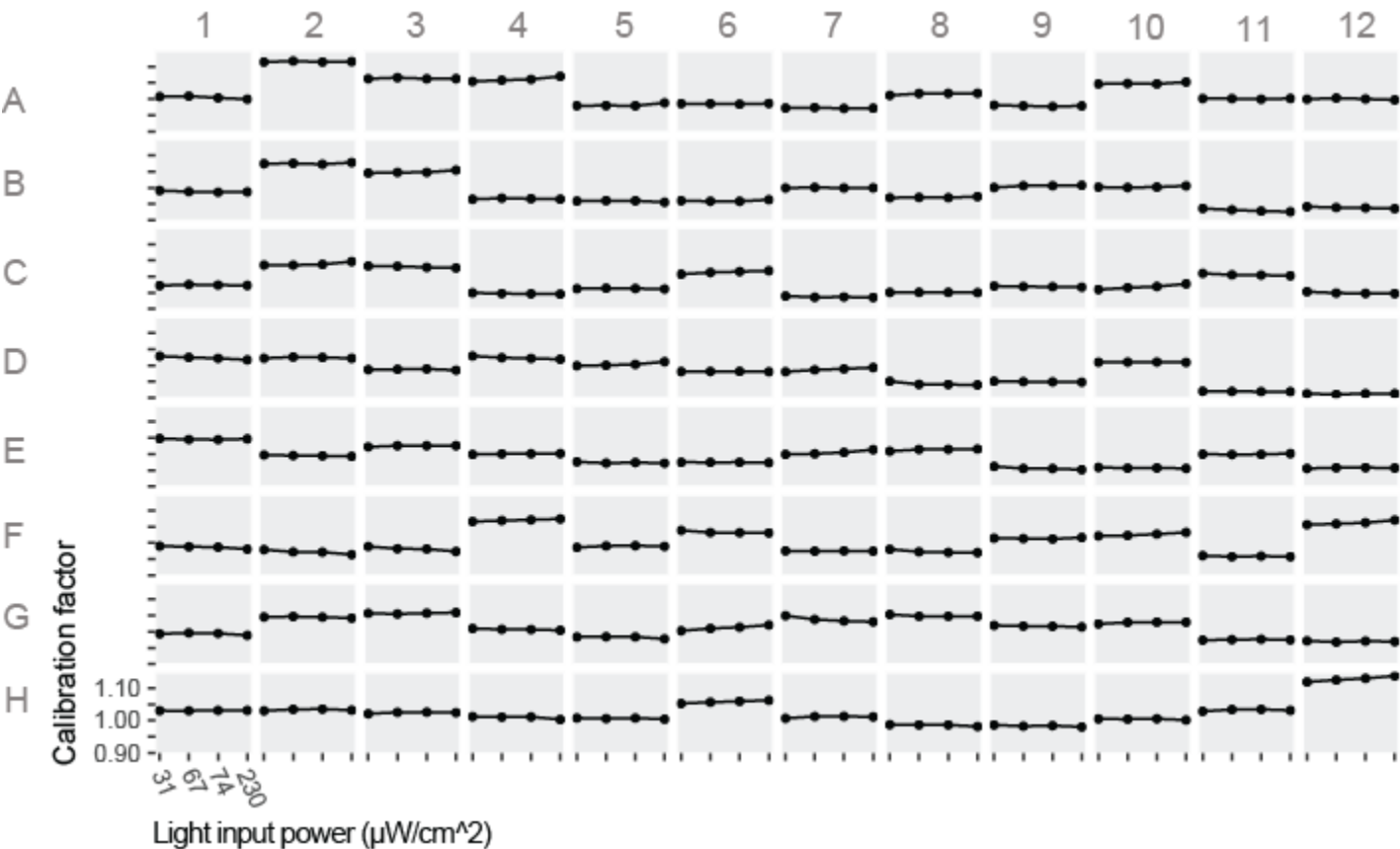
Supplementary Figure 3. Photodiode calibration factors are constant at different light input intensities. The calibration factor for each input intensity was calculated separately for each well at 4 different light intensities. In general, calibration factors were independent of input light power.

a

b
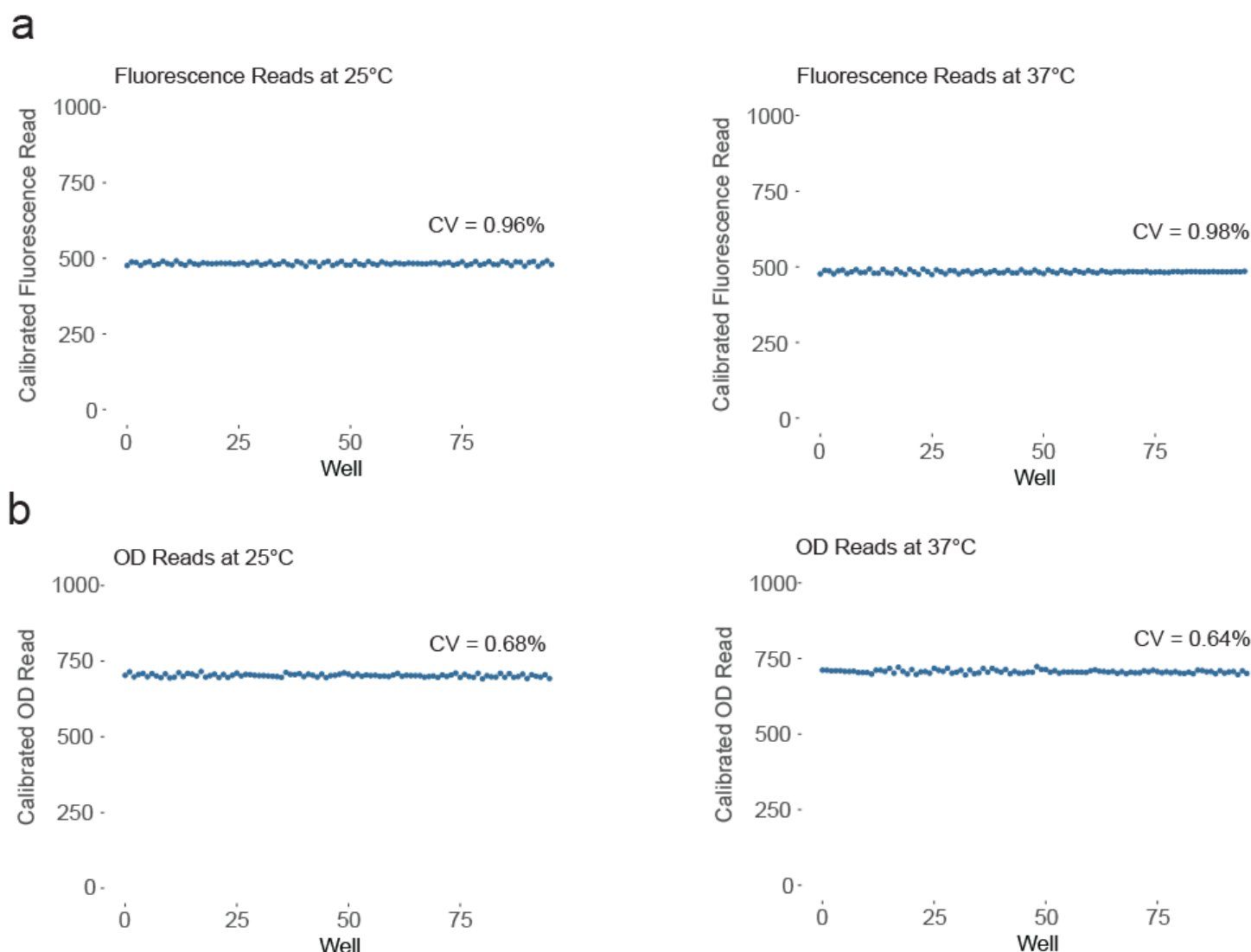
Supplementary Figure 4. Calibrated measurements do not vary as a function of temperature. a Calibrated fluorescence measurements were taken at 25°C using 40 µg/mL of lucifer yellow per well inside of a cell culture incubator. The cell culture incubator was then allowed to equilibrate at 37°C and measurements were repeated using the same calibration values. There was no significant change in measurement amplitude or variability of measurements between the two temperatures. **b** The same process was repeated for OD LED intensity with wells containing LB and again no significant temperature-dependent differences were observed.
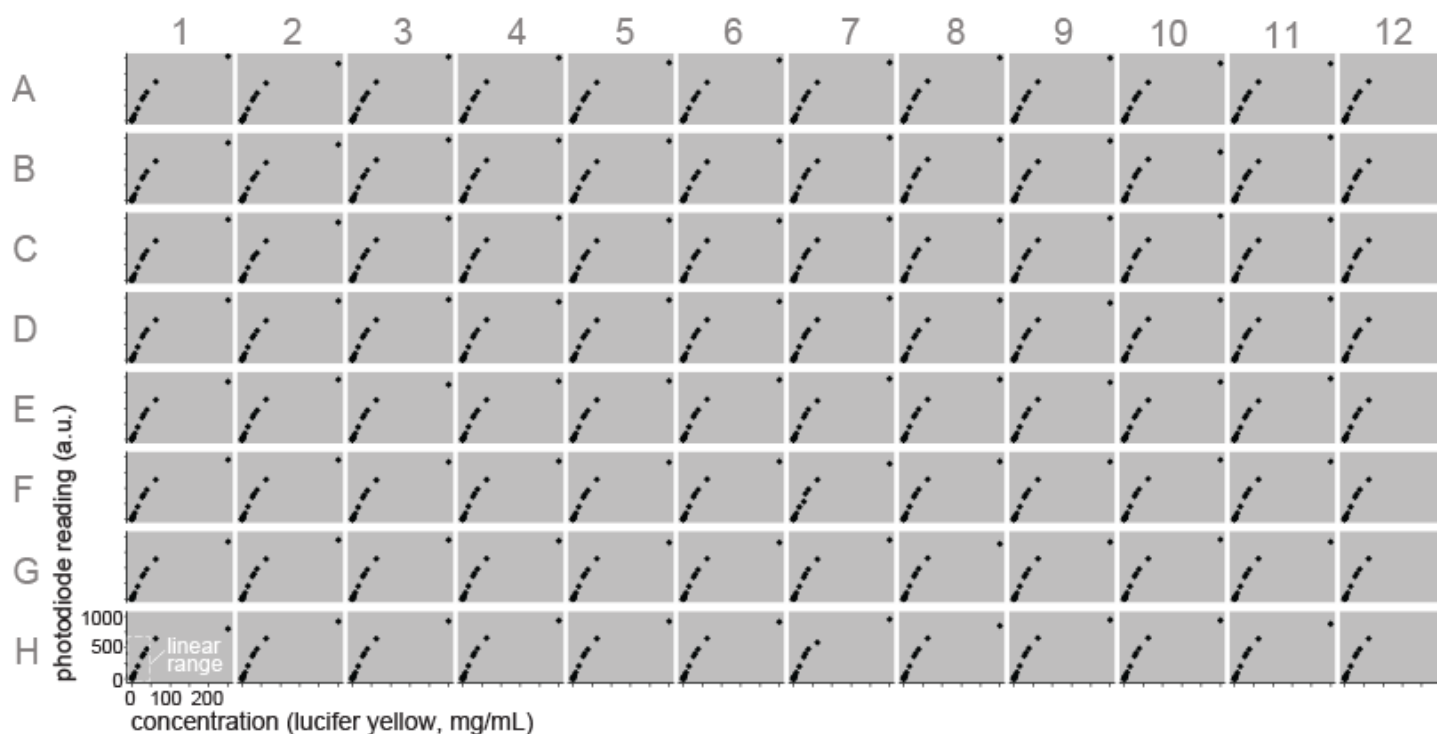
Supplementary Figure 5. Full range of photodiode fluorescence characterization

Fluorescence measurements of lucifer yellow dye were taken over a range of concentrations (2-250 µg/mL) in each of 96 wells in a calibrated oPR. Concentrations from 2-40 µg/mL are reproduced from **Figure 4**.

597
598
599
600
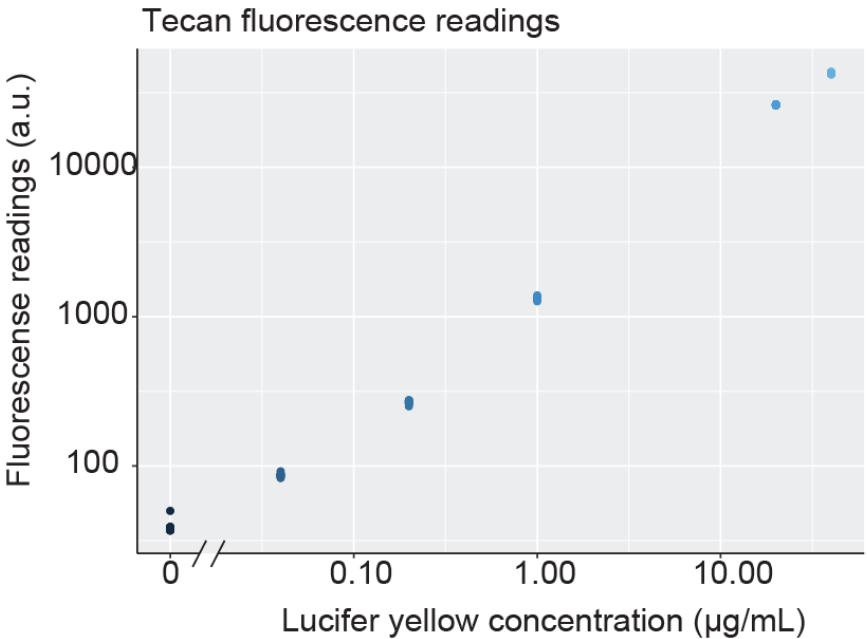
Supplementary Figure 6. Tecan limit of detection experiments. Lucifer yellow was diluted to several concentrations and measured using the Tecan Infinite M200. Based on this data, the limit of detection was calculated to be ~10 ng/mL. Each point represents the read from 1 well of lucifer yellow at the specified concentration.

606

607
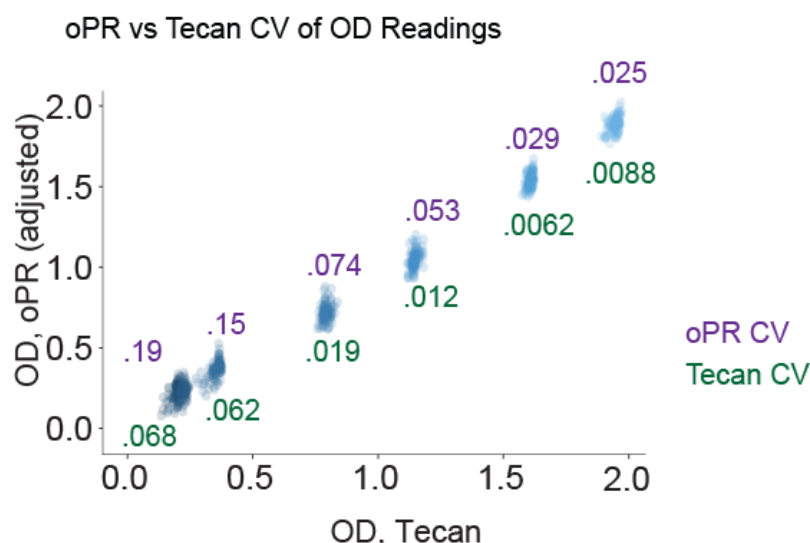
608 **Supplementary Figure 7. Coefficient of variation for oPR vs Tecan OD readings.** CV values were
609 calculated for data shown in **Figure B**. CVs displayed above data points correspond to oPR measurements
610 (magenta) at the corresponding concentration. CVs displayed below data points correspond to Tecan
611 measurements (green).

612

613
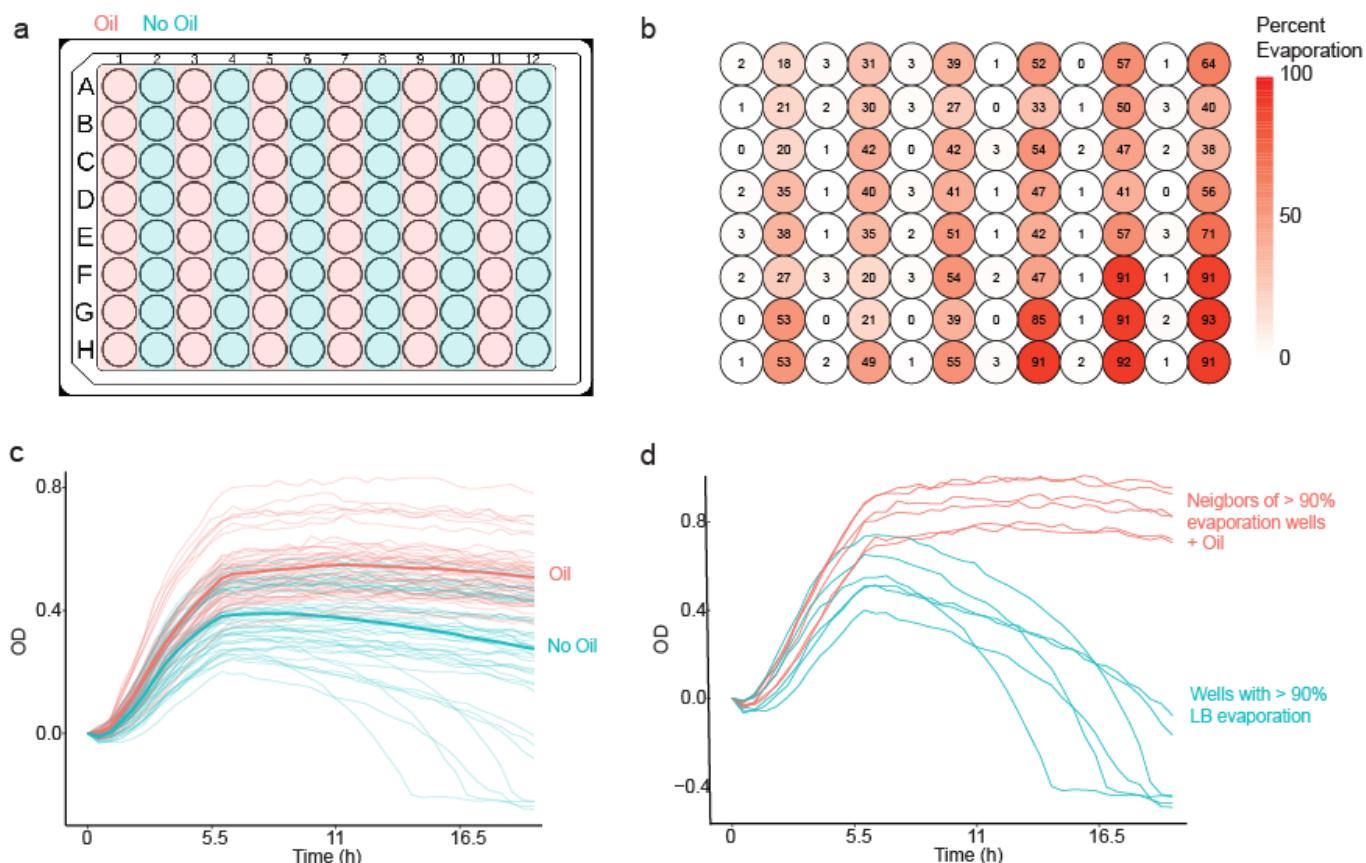
Supplementary Figure 8. Paraffin Oil prevents evaporation. a Bacteria were cultured in a 96-well plate with and without a 45 µL layer of paraffin oil for 18 hours of culture and measurement on an oPR with shaking at 1000rpm. **b** Percent LB evaporation from each well after the experiment described in (**a**). **c** OD readings over time from the experiment described in (**a**). Wells without paraffin oil exhibit an initial increase but subsequent decrease in OD readings, likely due to the fact that evaporation caused settling of dry residue on the outer edges of the well, creating an optically clear path through the center of the well, allowing greater light transmission than the initial liquid LB. By contrast, wells with paraffin oil exhibit a monotonic increase and plateau at ~ 6 hrs. **d** Examination of wells with most extreme evaporation compared to their neighbors with paraffin oil. Wells with >90% evaporation show a major decrease in OD readings over time (blue) while their direct oil-coated neighbors showed normal growth (red).
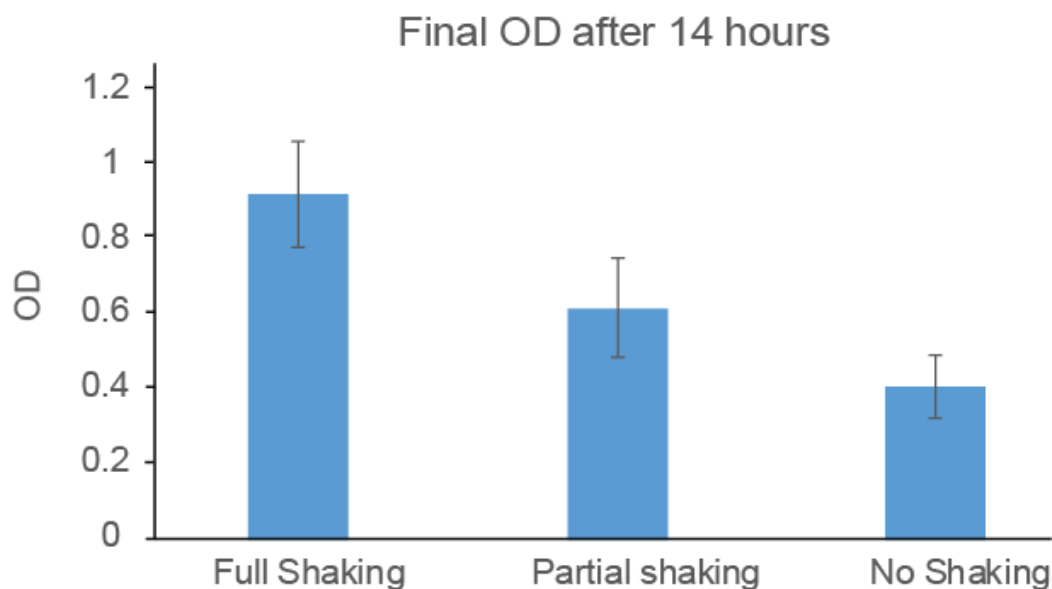
Supplementary Figure 9. Shaking effect on culture OD. Bacterial cultures were grown in 96 well plates for 14 hours with either constant shaking, 2 minutes of shaking every half hour, or no shaking. The final OD was measured, showing that increased shaking frequency led to higher final ODs. Each bar represents the mean of 96 wells with error bars representing 1 s.d.
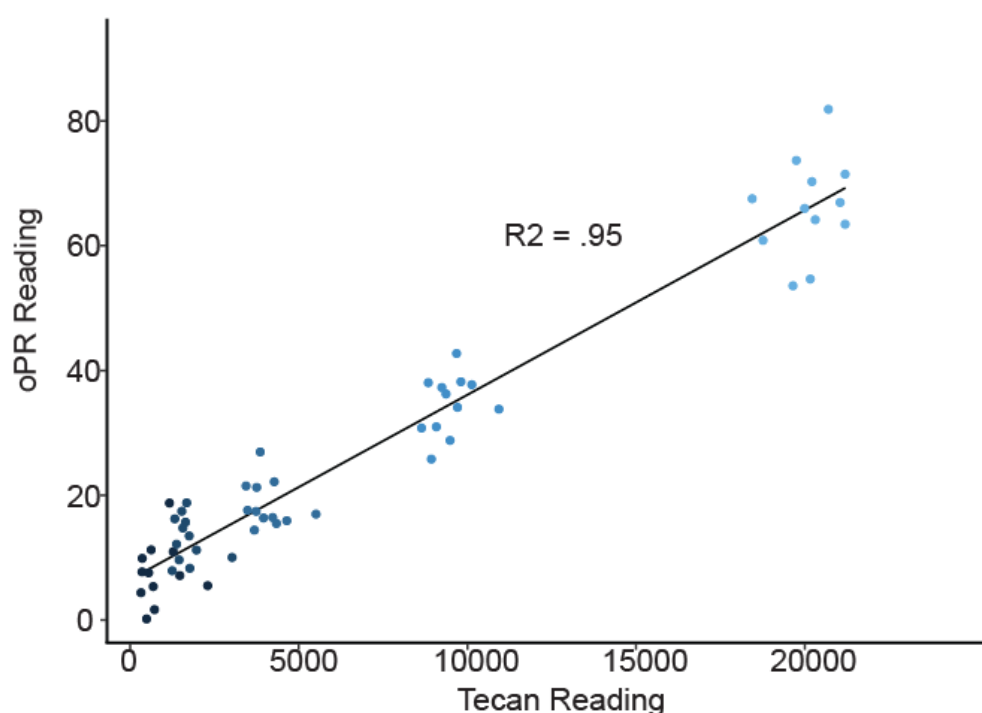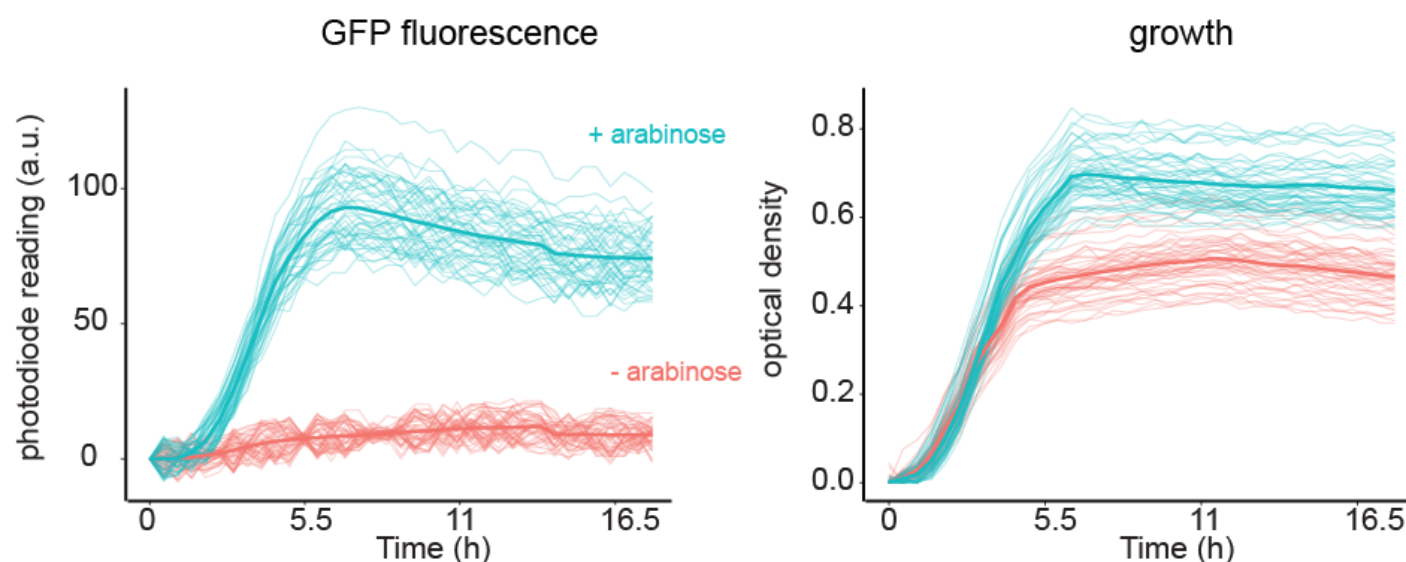
Supplementary Figure 10. oPR detection of GFP in live cultures. a Bacteria transformed with an arabinose inducible GFP expression plasmid were grown to saturation in 2 mL of LB + arabinose and diluted in a series of 2x dilutions. Each dilution was seeded in one row of a 96 well plate, and GFP intensities were read with both an oPR and Tecan. The oPR was able to detect GFP using a 475 nm excitation LED, and increases in fluorescence were linear with increases in fluorescence as measured by a Tecan plate reader. **b** Arabinose inducible GFP cultures were grown with or without arabinose for 18 hours, demonstrating the ability of the oPR to detect GFP expression during live time course experiments..

Methods

oPR Repository:

All files including 3D printed adapters, PCB designs, Arduino and Python scripts, assembly manuals, and usage manuals can be found in the attached **oPR repository**.

Circuit Design and CAD

All circuits and PCBs were designed using Kicad version 5.1.6-1. All CAD files for 3D printed adapters were designed using the Rhino software. All files are freely available in our online oPR repository.

oPR construction

oPR construction was achieved using standard PCB assembly protocols. The optoPlate was assembled as previously described[1] but with bi-color LEDs (Wurth Elektronik 150141RB73100) and a 589 nm OD LED (Broadcom HSMA-C380) used as the two LEDs for each well. The optoReader is a 2-sided PCB and was assembled as follows. Briefly, solder paste (Chipquik SMD4300AX250T3 183 °C) was deposited through a mask onto the top side of the PCB, which was fabricated by JLCPCB. Components were then placed and the PCB was baked in a toaster oven at 190 °C until solder paste became visibly melted. The PCB was allowed to cool to room temperature. Then, solder paste with a lower melting point (Chipquik TS391LT50 138 °C) was deposited via a mask on the bottom side of the PCB, components were placed, and the PCB was baked in a toaster oven at 150 °C until solder paste became visible melted. Detailed component placement diagrams can be found in our online repository (See first section of **Methods**). 2 layers of Rosco #312 filter sheets were used as emission filters for fluorescence detection. Each filter layer was cut using a Silhouette Cameo craft cutter using (cutting files are found in the oPR repository). The device acrylic base plate was laser cut using the laser cutting file also found in the file repository.

Experimental Conditions

For fluorescence calibration, a stock of Lucifer Yellow dye (Invitrogen, L453) was diluted in DI water to a concentration of 1 mg/mL, and was further diluted in water to the concentrations indicated. oPR fluorescence measurements were taken with 200 µL of dye solution in each well. For OD testing, 1.1 µm plastic beads (Millipore Sigma #LB11-1ML) were used to create standard dilutions for OD calibration. For each bead dilution, dilutions were added to a 96 well plate and moved directly to the oPR where OD was measured. The plate was then transferred to the TECAN, shaken for 10 seconds at 432 rpm, and OD was measured. For oPR experiments using bacterial samples, LB medium with the appropriate antibiotic was inoculated with bacteria, and 125 µL of the inoculated medium was seeded in each well of a 96-well plate and coated with 45uL of paraffin oil. 100 µL DI water was added to the space between wells to suppress sample evaporation. OD LEDs were calibrated at the start of each experiment with the starting (T = 0) cultures, representing the blank (max transmission). The blue LED intensity was programmed to stimulate the sample at an intensity of 1000 (~25% of max intensity) with a 30% duty cycle, stimulated for 3 second pulses with 7 second intervals of darkness between pulses. Pulsing was used to minimize potential phototoxicity. All experiments were carried out in a 37 °C incubator with shaking at 1000rpm.

Generation of pDawn/pDusk-mAmetrine E. coli:

pDawn and pDusk plasmid with a GFP reporter were a gift from Andreas Moeglich (Addgene plasmids #43796 and 43796). Arabinose inducible mAmetrine (pBad-mAmetrine) was a gift from Robert Campbell (Addgene plasmid # 18083). mAmetrine was inserted in place of GFP in both pDawn and pDusk plasmids via PCR and Gibson assembly (NEB HiFi mix). Using the same method, mAmetrine was replaced with GFP in the pBad-

693 mAmetrine plasmid to create arabinose inducible mAmetrine. Constructs were transformed into NEB DH5a
694 competent *E. coli.*
695
696 *Software*
697 To operate the optoPlateReader, a Python program communicates with two Arduinos, one on the optoPlate
698 and one on the optoReader. All software files and usage instructions can be found in our online oPR
699 repository**.**   Prior to the start of each experiment, the *optoReader.ino* and *optoPlate.ino* Arduino sketches are
700 uploaded individually to the respective Arduinos via USB. The *optoReader.ino* Arduino sketch operates the
701 optoReader Arduino and coordinates photodiode measurements and UV/excitation control. The *optoPlate.ino*
702 Arduino sketch operates the optoPlate and coordinates the blue and red (OD) LEDs. Next, the *Protocol.py* and
703 *GUI.py* scripts are opened on a central computer. The Arduino ports through which serial communication
704 occurs are hardcoded in the *Protocol.py* script and are edited accordingly where specified. The *Protocol.py*
705 program communicates with the two Arduinos. This program translates the user defined LED illumination
706 intensities, timing, reading intervals, and experimental duration into commands for the Arduinos. It also
707 receives photodiode measurements from each well, and it calculates user-defined feedback functions and
708 updates the oPR protocols in real time. The final step before running the experiment is to run *GUI.py*. This
709 script opens a graphical user interface that provides a user-friendly method to define the experimental
710 parameters that *Protocol.py* then feeds to the Arduinos. In the GUI, the user defines the groups of wells that
711 receive the same experimental conditions and then defines those conditions, including the stimulation light
712 intensity, duty cycle, and feedback functions. The user then specifies measurement parameters for
713 fluorescence and OD readings, including the frequency of measurement and the number of measurements to
714 average for one reading. After defining these conditions, the experiment is started by pressing the "Run Plate"
715 button. The two Arduinos remained connected to the computer through USB cables for the duration of the
716 experiment. For more details on software, see the usage manual found in our oPR repository.
717
718 *Calibration*
719 Calibration of the optoPlate components was essential to obtain precise measurements between all 96 wells
720 by ensuring consistent stimulation intensities and photodiode measurements. We first calibrated the
721 photodiodes to ensure consistent light measurements, and then we used the calibrated photodiodes to
722 calibrate all LED components. While photodiode calibration must be performed in the manner we describe
723 below, LED calibration can be performed through the GUI, which automates the steps described below.
724
725 To calibrate the photodiodes, a photo light box (Havox Hpb-40d) was used as a uniform light source to ensure
726 that each photodiode was illuminated with the same intensity of light. An external light meter (Thorlabs,
727 PM100D) was used to ensure uniformity across the illumination region (< 3% variation). The optoReader was
728 placed in the center of the light box, connected to the computer, and plugged into the power supply. No
729 adaptor or emission filter was used. The *optoReader_Manual.ino* script was uploaded and run to collect 100
730 readings per well for 96 wells. The following procedure was used to determine the calibration factor. First, the
731 mean of the 100 readings was calculated for each well. Then, the calibration factors for each well ($c_{i,pd}$) were
732 calculated by dividing the minimum reading of all wells by the average reading for that well:
733
734 $$(eq. 1) \quad c_{i,pd} = \min(r_{1-96})/r_i$$
735
736 Four calibration factors were calculated in this manner using four different illumination intensities (31,67, 74,
737 230 μW/cm^2) to ensure that the photodiode calibration was consistent across light intensities. Differing
738 illumination intensities were achieved by placing diffuser film between the light source and the oPR. The final
739 calibration factor for each photodiode was calculated by averaging the four calibration factors per well

740 (calculated for each irradiance value). However, calibration factors did not vary as a function of illumination
741 intensity (**Supplementary Figure 3**). The photodiode calibration factors were manually input to the Python
742 script, *Protocol.py*, during initial set-up of the oPR.
743
744 LED intensity on the optoPlate and optoReader is controlled by the TLC5947 LED driver chip (Texas
745 Instruments). Each chip controls intensity of up to 24 LEDs through 4095 intensity levels using pulse-wave
746 modulation (PWM). oPR LEDs were calibrated by calculating correction factors that were then applied to
747 adjust the PWM settings for each LED.
748
749 The stimulation (blue) LEDs were calibrated in the fully assembled oPR but without the excitation filter film,
750 which would have attenuated the blue light. An empty black, clear bottom 96-well plate (Greiner, #07000166)
751 was placed between the optoReader and optoPlate in order to calibrate the LEDs through air. To calibrate, the
752 script *optoReader_Manual.ino* was uploaded to the optoReader, and the script *optoPlate_Manual.ino* was
753 uploaded to the optoPlate. These scripts set the blue LED intensity to a value of 2000 to begin the calibration.
754 The optoReader reported the average of 100 readings per well of the 96 well array. The coefficient of variation
755 (CV, standard deviation/mean x 100%) of the readings was calculated. From these initial readings, a
756 calibration factor for each well ($c_{i,bl}$) was determined with the following formula:
757
758 $$(eq.\ 2)\quad c_{i,bl} = mean(r_{1-96})/r_i$$
759
760 where r is the mean reading from the optoReader. To test the calibration, the blue light intensities for each well
761 were multiplied by their calibration factor. These values were updated in the *optoPlate_Manual.ino* script,
762 which was uploaded to the optoPlate. A new set of readings was obtained, and the CV was calculated. This
763 process was iterated until the CV reached < 1%, or up to 3 rounds (no decrease in CV was observed after 3
764 rounds). The final blue LED calibration factors were saved to a .csv file through the GUI and manually added to
765 the *optoPlate.ino* Arduino script at the initial set-up of the oPR.
766
767 The optical density (OD, red) LEDs were calibrated in a similar manner to the blue LEDs above, with a few key
768 differences. First, the OD LEDs were calibrated such that the OD readings were consistent between wells. This
769 means that calibration normalizes not just LED intensity, but also slight variations in alignment and light scatter
770 that can occur between wells. To achieve this, calibration must be performed with liquid in each well, since the
771 optical properties of the sample liquid can differentially scatter the red light. Second, OD LED calibration was
772 performed at the beginning of every experiment to account for differences in liquid volume, clarity, meniscus,
773 etc. from experiment to experiment (other LEDs were only calibrated once after initial construction of the oPR
774 device). To begin calibration, a black, clear bottom 96-well was filled with 200 μL of LB in each well, and the
775 full oPR was assembled. The script *optoPlate_Manual.ino* set the OD LEDs to an initial brightness setting of
776 500. The optoReader reported the average of 100 readings per well. The CV of the measurements was
777 calculated, and the calibration factors for each well ($c_{i,OD}$) were calculated using the following equation:
778
779 $$(eq.\ 3)\quad c_{i,OD} = mean(r_{1-96})/r_i$$
780
781 As before, the calibration factors were used to adjust the OD LED intensity settings. These adjusted values
782 were then uploaded to the optoPlate, and new measurements were taken. This measurement/adjustment cycle
783 was performed iteratively until the CV of the readings reached < 1%, or for up to three rounds. The final OD
784 LED calibration factors were saved through the GUI as a .csv file and were referenced by the *Protocol.py*
785 program throughout the experiment.
786

787 The UV LEDs were calibrated based on the measured oPR fluorescence of a uniform concentration of
788 fluorescent dye, lucifer yellow, which has excitation and emission spectra comparable to mAmetrine. To begin
789 calibration, 200 µL of 1000 µg/mL lucifer yellow diluted in water were deposited in each well of a clear-bottom,
790 black-walled plate, and the oPR was fully assembled. The script *optoReader_Manual.ino* was modified to set
791 the UV LEDs to a maximum intensity setting (4095), and the script was uploaded to the optoReader Arduino.
792 The optoPlate was mounted over the well-plate as usual, but no script was uploaded to the optoPlate Arduino
793 since none of its components were required for UV LED calibration. Photodiode measurements were recorded
794 as before, and calibration factors ($c_{i,UV}$) were determined with the following equation:
795
796 $$\text{(eq. 4)} \quad c_{i,UV} = \min(r_{1\text{-}96})/r_i$$
797
798 LED intensities were adjusted and measured, and this process was iterated as for the other LEDs. The final
799 UV LED calibration factors were manually added to *optoReader.ino* at the initial set-up of the oPR.
800
801 *Correcting OD values to match Tecan plate reader*
802 Comparison of OD from the oPR and Tecan found that, while data from both instruments were ~linearly
803 related, the absolute magnitudes of readings from the oPR vs Tecan varied by ~2-fold (**Figure 5B).** To bring
804 oPR readings in line with industry-standard Tecan readings, a transform function was generated that related
805 oPR OD readings to expected Tecan readings. During experiments, oPR OD readings were passed through
806 the inverse of this equation to generate final adjusted readings. The lines of best fit for the per-well data in
807 **Figure 5B** were generated in R using the code:
808
809 $$\text{lm(log(ReadingOPR+1) ~ ReadingTECAN, WellDataSet)}$$
810
811 where lm() generates a line of best fit between log(ReadingOPR+1) and ReadingTECAN, and ReadingOPR
812 represents OD readings at all concentrations for a single well. ReadingTECAN represents all Tecan readings
813 for that same well, and WellDataSet is the data frame that these well values are stored within. A logarithmic
814 transformation was used because it was empirically found to provide a better fit to the data, particularly at
815 lower ODs. This formula generates the slope (m) and y-intercept (b) for that well which can then be applied to
816 oPR OD readings (r) from the same well in future experiments using the following formula to generate TECAN
817 adjusted results (c).
818
819 $$\text{(eq. 5)} \quad c = \frac{log(r+1)-b}{m}$$
820
821 Slopes and y-intercepts can then be entered into the FeedbackFuncs.py file in order to utilize real time
822 correction of oPR OD data for feedback enabled experiments. For experiments that do not require feedback,
823 OD correction can be applied after completion of the experiment when processing OD outputs.
824
825
826

References

1. Bugaj, L. J. & Lim, W. A. High-throughput multicolor optogenetics in microwell plates. *Nat. Protoc.* **14**, 2205–2228 (2019).

2. Repina, N. A., McClave, T., Bao, X., Kane, R. S. & Schaffer, D. V. Engineered illumination devices for optogenetic control of cellular signaling dynamics. *bioRxiv* 675892 (2019) doi:10.1101/675892.

3. Gerhardt, K. P. *et al.* An open-hardware platform for optogenetics and photobiology. *Sci. Rep.* **6**, 35363 (2016).

4. Hannanta-Anan, P. & Chow, B. Y. Optogenetic Control of Calcium Oscillation Waveform Defines NFAT as an Integrator of Calcium Load. *Cell Syst* **2**, 283–288 (2016).

5. Kyriakakis, P. *et al.* Building a Simple and Versatile Illumination System for Optogenetic Experiments. *J. Vis. Exp.* (2021) doi:10.3791/61914.

6. Höhener, T. C., Landolt, A., Dessauges, C., Gagliardi, P. A. & Pertz, O. LITOS - a versatile LED illumination tool for optogenetic stimulation. *bioRxiv* 2022.03.02.482623 (2022) doi:10.1101/2022.03.02.482623.

7. Johnson, Z. I. & Sheldon, T. L. A high-throughput method to measure photosynthesis-irradiance curves of phytoplankton. *Limnol. Oceanogr. Methods* **5**, 417–424 (2007).

8. Chen, M., Mertiri, T., Holland, T. & Basu, A. S. Optical microplates for high-throughput screening of photosynthesis in lipid-producing algae. *Lab Chip* **12**, 3870–3874 (2012).

9. Höhener, T. C. *et al.* LITOS: a versatile LED illumination tool for optogenetic stimulation. *Sci. Rep.* **12**, 1–11 (2022).

10. Carrasco-López, C., García-Echauri, S. A., Kichuk, T. & Avalos, J. L. Optogenetics and biosensors set the stage for metabolic cybergenetics. *Curr. Opin. Biotechnol.* **65**, 296–309 (2020).

11. Kumar, S., Rullan, M. & Khammash, M. Rapid prototyping and design of cybergenetic single-cell controllers. *Nat. Commun.* **12**, 5651 (2021).

12. Toettcher, J. E., Gong, D., Lim, W. A. & Weiner, O. D. Light-based feedback for controlling intracellular signaling dynamics. *Nat. Methods* **8**, 837–839 (2011).

13. Milias-Argeitis, A., Rullan, M., Aoki, S. K., Buchmann, P. & Khammash, M. Automated optogenetic

854   feedback control for precise and robust regulation of gene expression and cell growth. *Nat. Commun.* **7**,

855   12546 (2016).

856   14. Harrigan, P., Madhani, H. D. & El-Samad, H. Real-Time Genetic Compensation Defines the Dynamic

857   Demands of Feedback Control. *Cell* **175**, 877–886.e10 (2018).

858   15. Soffer, G., Perry, J. M. & Shih, S. C. C. Real-Time Optogenetics System for Controlling Gene Expression

859   Using a Model-Based Design. *Anal. Chem.* **93**, 3181–3188 (2021).

860   16. Steel, H., Habgood, R., Kelly, C. L. & Papachristodoulou, A. In situ characterisation and manipulation of

861   biological systems with Chi.Bio. *PLoS Biol.* **18**, e3000794 (2020).

862   17. Richter, F. *et al.* Upgrading a microplate reader for photobiology and all-optical experiments. *Photochem.*

863   *Photobiol. Sci.* **14**, 270–279 (2015).

864   18. Szymula, K. P. *et al.* An Open-Source Plate Reader. *Biochemistry* **58**, 468–473 (2019).

865   19. Jensen, P. A., Dougherty, B. V., Moutinho, T. J., Jr & Papin, J. A. Miniaturized plate readers for low-cost,

866   high-throughput phenotypic screening. *J. Lab. Autom.* **20**, 51–55 (2015).

867   20. Ai, H.-W., Hazelwood, K. L., Davidson, M. W. & Campbell, R. E. Fluorescent protein FRET pairs for

868   ratiometric imaging of dual biosensors. *Nat. Methods* **5**, 401–403 (2008).

869   21. Stevenson, K., McVey, A. F., Clark, I. B. N., Swain, P. S. & Pilizota, T. General calibration of microbial

870   growth in microplate readers. *Sci. Rep.* **6**, 38828 (2016).

871   22. Kim, S. *et al.* Optimizing E. coli as a formatotrophic platform for bioproduction via the reductive glycine

872   pathway. *Front. Bioeng. Biotechnol.* **11**, 1091899 (2023).

873   23. Desai, T. A. & Rao, C. V. Regulation of Arabinose and Xylose Metabolism in Escherichia coli. *Appl.*

874   *Environ. Microbiol.* **76**, 1524 (2010).

875   24. Ohlendorf, R., Vidavski, R. R., Eldar, A., Moffat, K. & Möglich, A. From dusk till dawn: one-plasmid

876   systems for light-regulated gene expression. *J. Mol. Biol.* **416**, 534–542 (2012).

877   25. Zhao, E. M. *et al.* Optogenetic regulation of engineered cellular metabolism for microbial chemical

878   production. *Nature* **555**, 683–687 (2018).

879   26. Zhang, Y. *et al.* Biosensor for branched-chain amino acid metabolism in yeast and applications in

880   isobutanol and isopentanol production. *Nat. Commun.* **13**, 270 (2022).

881 27. Grødem, E. O., Sweeney, K. & McClean, M. N. Automated calibration of optoPlate LEDs to reduce light

882   dose variation in optogenetic experiments. *Biotechniques* **69**, 313–316 (2020).

883 28. Thomas, O. S., Hörner, M. & Weber, W. A graphical user interface to design high-throughput optogenetic

884   experiments with the optoPlate-96. *Nature protocols* vol. 15 2785–2787 (2020).

885